

AD-A050 293

NAVAL OCEAN SYSTEMS CENTER SAN DIEGO CA  
A TECHNIQUE FOR OBTAINING D-REGION ELECTRON DENSITY PROFILES FR--ETC(U)  
NOV 77 D G MORFITT, C H SHELLMAN

F/6 20/14

DNA-MIPR-77-521

UNCLASSIFIED

NOSC/IR-781

NL

| OF |  
AD  
A050293



END  
DATE  
FILMED  
3-78  
DDC

ADA 050293

1  
2  
0.5

# A TECHNIQUE FOR OBTAINING D-REGION ELECTRON DENSITY PROFILES FROM VLF REFLECTION COEFFICIENTS.

*Interim Report No. 781*

DG Morfill and CH Shellman

AD NO. 100-10000  
AMF FILE COPY



NAVAL OCEAN SYSTEMS CENTER  
ELECTROMAGNETIC PROPAGATION DIVISION  
SAN DIEGO, CALIFORNIA 92132

100-10000-1077

## UNCLASSIFIED

SECURITY CLASSIFICATION OF THIS PAGE (When Data Entered)

REPORT DOCUMENTATION PAGE		READ INSTRUCTIONS BEFORE COMPLETING FORM
1. REPORT NUMBER Interim Report No. 781	2. GOVT ACCESSION NO. NOSC/IR-781	3. RECIPIENT'S CATALOG NUMBER
4. TITLE (and Subtitle) A Technique For Obtaining D-Region Electron Density Profiles From VLF Reflection Coefficients.		5. TYPE OF REPORT & PERIOD COVERED Research Report
6. AUTHOR(s) David G. Morfitt Charles H. Shellman	7. PERFORMING ORG. REPORT NUMBER	
8. CONTRACT OR GRANT NUMBER(s) DNA-MIPR-77-521 DNA-MIPR-78-504	9. PERFORMING ORGANIZATION NAME AND ADDRESS Naval Ocean Systems Center 271 Catalina Blvd. San Diego, CA 92152	
10. PROGRAM ELEMENT, PROJECT, TASK & WORK UNIT NUMBERS DNA S99QAXH B042 NOSC MP20		11. REPORT DATE 16 Nov 1977
12. NUMBER OF PAGES 91		13. SECURITY CLASS. (of this report) UNCLASSIFIED
14. MONITORING AGENCY NAME & ADDRESS (if different from Controlling Office)		
15. SECURITY CLASSIFICATION SCHEDULE		
16. DISTRIBUTION STATEMENT (of this Report) Approved for public release; distribution is unlimited.		
17. DISTRIBUTION STATEMENT (of the abstract entered in Block 20, if different from Report)		
18. SUPPLEMENTARY NOTES		
19. KEY WORDS (Continue on reverse side if necessary and identify by block number) VLF Propagation Electron density profiles Ionosphere      Inversion Reflection coefficients		
20. ABSTRACT (Continue on reverse side if necessary and identify by block number) A technique is described for determining D-region electron density profiles from VLF reflection coefficients. Some of the problems concerning convergence of the iterative scheme are discussed as well as the constraints introduced to account for features of the profile for which information is not provided by reflection coefficient data. Also, an example is given where the technique is applied using simulated data.		

## TABLE OF CONTENTS

	Page
ABSTRACT	1
I INTRODUCTION	2
II GENERAL BACKGROUND	7
(A) Inversion Without Smoothing	7
(B) Smoothing With No Inversion	9
1. General case	9
2. Limiting case of interpolation between data points	16
(C) Combination Problem of Smoothing and Inversion	19
III DETERMINATION OF ELECTRON DENSITY PROFILES FROM VLF REFLECTION COEFFICIENTS	30
(A) Reflection Coefficient Data	30
(B) The Ionospheric Model	33
(C) Computation of Ionospheric Reflection Coefficients	34
(D) Comparison of Data with Computed Reflection Coefficients	35
(E) Application of the Combined Smoothing and Inversion Techniques to the Ionosphere Problem	36
(F) Characteristics of the Solution of Equations in Terms of the "r( $\omega$ )" Parameter	41
(G) Transformation Function , "g(r, $\omega$ )"	43
(H) The Derivatives , $(dr/d\omega)_i$ and $(dR/d\omega)_i$	46
(I) Following of the Phase Angle, $\phi$ , Along the Curve $g(\omega)$ [or $G(\omega)$ ], and Derivation of the Derivatives, $(\partial g(\omega_i)/\partial \alpha_j)$	50
IV SUMMARY OF THE INVERSION TECHNIQUE WITH EXAMPLE USING SIMULATED DATA	52
V FIGURES	56
VI REFERENCES	66
VII APPENDICES	67
(A) The "C" Matrix	67
(B) The Derivative of the Curvature Term "c"	71
(C) The Derivative Terms, $(dy/dx)_j$	73
(D) The Uncertainty Matrix, $[1/\sigma]$	77
(E) The Derivatives, $(\partial g_i/\partial r_j)$	84

ACCESSION NO.	
NTIS	White Section <input checked="" type="checkbox"/>
000	Buff Section <input type="checkbox"/>
UNANNOUNCED	
JSTIFICATION	
BY	
DISTRIBUTION/AVAILABILITY CODES	
SPL.	AVAIL. END. OR SPECIAL
A	

## ABSTRACT

A technique is described for determining D-region electron density profiles from VLF reflection coefficients. Some of the problems concerning convergence of the iterative scheme are discussed as well as the constraints introduced to account for features of the profile for which information is not provided by reflection coefficient data. Also, an example is given where the technique is applied using simulated data.

## I. INTRODUCTION

Radio sounding at very low frequencies (VLF - 3 to 30 kHz) is a valuable method for exploring the lowest ionosphere. With special sounding techniques, such as described in reference 1, it is possible to obtain continuous sounding data simultaneously at many frequencies over the VLF band. However, considerable difficulty is encountered in attempts to obtain quantitative information concerning ionospheric properties from the sounding observations. The theory of radio wave reflection from an inhomogeneous, anisotropic plasma such as the ionosphere is rather well developed, so that if the properties of the ionosphere are known, it is possible to calculate the expected effects on the radio waves. The real problem to be solved, however, is the inverse problem of determining the unknown ionospheric properties from the observed effects on the radio waves. The use of data in this manner to obtain electron-density distributions of the ionosphere has become known as profile inversion.

Early work in ionospheric inversion (e.g. references 2 and 3) used trial and error techniques to deduce profiles. That is, values for the ionospheric properties were assumed and the ionospheric reflection coefficients calculated; these were then compared with experimental values, and if the agreement was not satisfactory, the calculations were performed again with different values for the ionospheric properties. The goodness of fit between the calculations and the experimental data were determined only by a subjective estimate of the investigator.

There has long been a question as to whether VLF radio propagation data might be readily inverted to obtain D-region electron density distributions, without the use of trial-and-error. There has also been a question as to whether profiles, if found to fit the data, could be claimed to be unique.

In this report a method of search is proposed for investigating the problem.

In the case of steep-incidence sounding the measured data are elements of the ionosphere reflection matrix at several experimental frequencies. If an electron density profile is known, or assumed, the elements of the reflection matrix may be computed in a straightforward manner by use of a full-wave solution, such as that given by Budden, reference 4. The inversion problem is to begin with reflection coefficient data and deduce the electron density profile.

Many of the fundamental ideas of the inversion technique described in this report were previously presented in reference 5. For this reason, several references will be made to that report rather than to reproduce the material.

The approach taken in searching for a best-fit electron density profile from data is that the profile is to be linear (on a log scale) unless the data gives information to justify a given degree of detail. To carry out this approach, two functions are defined. The first is a measure of deviation of computed reflection coefficients from data, defined as:

$$S = \sum_i^m \left\{ \left( r_i - R_i \right) / \sigma_i \right\}^2 \quad (1)$$

where

$m$  - is the number of propagation frequencies

$r_i$  - are the computed values of the reflection coefficients

$R_i$  - are the reflection coefficient data

$\sigma_i$  - are the uncertainties in the data values.

The second function is a measure of detail, or curvature, in the profile and is defined as:

$$c = \int \left\{ \frac{d^2 \log N_e}{dz^2} \right\}^2 dz \quad (2)$$

where  $N_e$  is the electron density,  $z$  is the height variable and the integral is taken over the range of the profile.

The required profile is sought by an iterative technique in which the total curvature in the profile is allowed to increase in steps to improve the fit to data. Each step requires a perturbation-type solution in which the full-wave solution of Budden is analytically differentiated with respect to perturbations in the profile.

The end result sought in using the inversion procedure is the determination of a profile which contains all the detail justified by the data, but which does not contain spurious detail which would represent fitting to error in the data. There should be an optimum trade-off between deviation from data, represented by the value of  $s$ , and curvature in the profile, represented by the value of  $c$ . The trade-off may be represented by the condition:

$$c + \lambda s \rightarrow \min \quad (3)$$

where the value of  $\lambda$  must be chosen for the optimum condition.

A solution to (3) may easily be found for  $\lambda=0$ . A solution which is first order in  $r_i$  may then be used to obtain a solution for a small value

of  $\lambda$ . The first-order solution may then be used to find profiles for successively larger values of  $\lambda$ . As the search proceeds, the profile will, in general, develop more detail and the fit to data will improve until a singularity is encountered in the solution.

This report is divided into three major sections other than the Introduction. Section II is a discussion of the general background needed for understanding the ideas of smoothing and inversion. Section III describes the procedure for obtaining the electron density profile from reflection coefficient data. Section IV summarizes the inversion scheme and gives an example using simulated data.

The notation used throughout this report is as described below. In general the subscript convention used is that  $j$  and  $j'$  refer to the " $n$ " layers of the electron density profile while  $i$  and  $i'$  refer to the " $m$ " data parameters. Note that most equations are written so that subscripted variables may be thought of as matrices or vectors.

The notation is:

Square matrix:

$$\tilde{A} = \begin{pmatrix} a_{11} & \cdots & a_{1n} \\ \vdots & \ddots & \vdots \\ a_{n1} & \cdots & a_{nn} \end{pmatrix} = \begin{matrix} j' \rightarrow \\ \downarrow \\ j \end{matrix} \begin{pmatrix} a_{jj'} \end{pmatrix} \quad (4, a)$$

Rectangular matrix:

$$\tilde{B} = \begin{bmatrix} b_{11} & \cdots & b_{1m} \\ \vdots & \ddots & \vdots \\ b_{n1} & \cdots & b_{nm} \end{bmatrix} = \begin{matrix} i \rightarrow \\ \downarrow \\ j \end{matrix} \begin{bmatrix} b_{ji} \end{bmatrix} \quad (4, b)$$

Column vector:

$$\vec{C} = \begin{pmatrix} c_1 \\ \vdots \\ c_n \end{pmatrix} = \overset{j}{\downarrow} \begin{pmatrix} c_j \end{pmatrix} \quad (4, c)$$

Row vector:

$$\vec{D} = \overbrace{d_1 \cdots d_n}^j = \overbrace{d_j}^{\vec{j}} \quad (4, d)$$

## II. GENERAL BACKGROUND

### A. Inversion Without Smoothing

A simple inversion technique is illustrated by the Newton-Raphson iteration procedure. The problem is to find "x" such that:

$$f(x) = F \text{ (i.e. a constant)} \quad (5)$$

Consider figure 1 as an example where the curve for  $f(x)$  is given by the arc PQ. The solution for "x" is obtained by starting with an initial value for "x" (e.g.  $x = x_0$ ). This gives, from figure 1:

$$\frac{F - f(x_0)}{(x_1 - x_0)} = \left. \frac{df}{dx} \right|_{x=x_0} \quad (6)$$

or let

$$\Delta f_1 = (F - f(x_0)) \quad (7)$$

and

$$\Delta x_1 = (x - x_0) = \left. \left( \frac{df(x)}{dx} \right)^{-1} \right|_{x=x_0} \cdot \Delta f_1 \quad (8)$$

This leads to an approximate value of "x" for  $f(x) = F$ , given by:

$$x_1 = x_0 + \Delta x_1 \quad (9)$$

The iterative procedure is then repeated with:

$$\left. \begin{array}{l} \Delta f_i = F - f(x_{i-1}) \\ \Delta x_i = \left( \frac{df(x)}{dx} \right)^{-1} \Big|_{x=x_{i-1}} \cdot \Delta f_i \end{array} \right\} \quad (10)$$

and

$$x_i = x_{i-1} + \left( \frac{df(x)}{dx} \right)^{-1} \Big|_{x=x_{i-1}} \cdot \Delta f_i \quad (11)$$

until convergence occurs when  $\Delta f$  becomes less than some pre-assigned tolerance value. Figure 1 illustrates the iterative process.

The technique will yield the wanted solution for "x" provided that the slope of the curve does not become zero along the arc QP of figure 1.

Figure 2 shows an example of a curve,  $f(x)$ , where the inversion technique will not converge because of the zero slope of the curve at the point  $x_3$ .

Next, a modified version of the Newton-Raphson iteration scheme is considered. In this case it is desired to follow the curve  $f(x)$ , from an initial chosen value of "x", as  $f(x)$  approaches the fixed value,  $F$ . This situation is important in that it serves as an analogy for more complex cases.

The problem is to find "x" such that  $f(x) = F$  (a constant). The solution for the  $i$ -th step is:

$$\Delta x_i = (x_i - x_{i-1}) = \left( \frac{df(x)}{dx} \right)^{-1} \Big|_{x_{i-1}} \cdot (\bar{F}(\lambda_i) - f(x_{i-1})) \quad (12)$$

where

$$\bar{F}(\lambda_i) = F - (F - f(x_{i-1})) \cdot e^{-\lambda_i} \quad (13)$$

and where " $\lambda_i$ " takes on values monotonically increasing from 0 to  $\infty$ .

It is seen from figure 3 that the steps converge to the value  $f(x) = F$  only if  $f(x)$  is a monotonic function of "x". If this is not the case, the steps will not converge. Even in this case, however, there may exist another function  $g(x) = \text{function}(f(x))$  which is a monotonic function of "x". The above curve-following procedure may then be used with  $g(x)$  to converge to a value  $G = \text{function}(F)$ . This point is important in making analogies with more complex inversion problems.

#### B. Smoothing With No Inversion

##### 1. General Case.

When data of the form  $y(x)$  vs.  $x$  is considered, it is common practice to "smooth out" experimental error by drawing a smooth curve close to, but not necessarily through, the data points. The object is to draw a curve which contains all the detail justified by the data, but which does not contain spurious detail which would represent fitting to error in the data.

Figure 4 illustrates a set of data points to be examined. The method of smoothing, presented here, is a technique for drawing a smooth curve  $y(x)$  close to a set of data points  $Y_i = Y(X_i)$ . In this technique the condition specifying the smooth curve  $y(x)$  is given by:

$$C + \lambda S \longrightarrow m/m \quad (14)$$

where "c" is the curvature and "s" is a measure of deviation of the curve,  $y(x)$  from the data points. The parameter " $\lambda$ " specifies the trade-off between fit to data and smoothness of the curve  $y(x)$ .

The measure of deviation of the curve,  $y(x)$  from the data points is given by:

$$S = \sum_{i=1}^m \left\{ \frac{y(X_i) - Y(X_i)}{\sigma_i} \right\}^2 \quad (15)$$

The  $Y_i = Y(X_i)$  are data values and the  $y(X_i)$  are values of the curve  $y(x)$  at the coordinates,  $x = X_i$ . The  $\sigma_i$  are the uncertainties in the data values.

In matrix notation, equation (15) is written as:

$$S = \underbrace{\frac{y(X_i) - Y(X_i)}{\sigma_i}}_{i \rightarrow} \cdot \underbrace{i \left( \frac{y(X_i) - Y(X_i)}{\sigma_i} \right)}_{\downarrow} \quad (16)$$

where both right hand factors are vectors. Also,  $i = 1, \dots, m$ ; where "m" is the number of data points.

Differentiation of equation (16) with respect to  $y(X_i)$  gives:

$$\frac{d}{dY(X_i)} \left( \frac{\partial S}{\partial Y(X_i)} \right) = -2 \cdot \left( \frac{y(X_i) - Y(X_i)}{\sigma_i^2} \right) \quad (17)$$

The curvature term "c" is defined by:

$$c = \int \left( \frac{d^2y}{dx^2} \right)^2 dx \quad (18)$$

Equation (14) defines the entire curve,  $y(x)$ . However, in practice,  $y(x)$  can only be determined at a finite number of points,  $x_j$ . For simplicity it will be assumed that the  $x_j$ 's are equally spaced at intervals,  $\Delta x$ , and that each  $X_i$  is coincident with an  $x_j$ . From appendix A the second derivative at  $x_j$  is approximated by:

$$\frac{d^2y}{dx^2} \approx \left( \frac{y_{j+1} - y_j}{\Delta x} - \frac{y_j - y_{j-1}}{\Delta x} \right) / \Delta x \quad (19)$$

The curvature function "c" is then:

$$c \approx \left\{ \sum_{j=2}^{n-1} (y_{j+1} - 2y_j + y_{j-1})^2 \right\} / (\Delta x)^3 \quad (20)$$

where  $n$  is the number of points,  $x_j$ . This can be written in matrix notation as:

$$c = (\Delta x)^{-3} \underbrace{\frac{j}{y_j}}_{\text{Diagram: } j \rightarrow y_j} \cdot j \left( C_{j'j} \right) \cdot j \left( y_j \right) \quad (21)$$

where the  $C_{j,j}$  are elements of the matrix

$$\xi = \begin{pmatrix} 1 & -2 & 1 \\ -2 & 5 & -4 & 1 \\ 1 & -4 & 6 & -4 & 1 \\ & & & & \\ & & 1 & -4 & 6 & -4 & 1 \\ & & 1 & -4 & 5 & -2 \\ & & 1 & -2 & 1 \end{pmatrix} \quad (22)$$

The derivation of this  $C$  matrix is given in appendix A.

The derivative of the curvature term, "c", with respect to each  $y_j$  is derived in appendix B to be:

$$\frac{\partial C}{\partial y_i} = 2/(4N^p) \cdot \underbrace{y_i}_{\downarrow} \cdot \underbrace{\left( C_{i,i} \right)}_{\uparrow} \quad (23)$$

The condition for the minimization of equation (14) is:

$$\frac{\partial C}{\partial y(x_i)} + \lambda \frac{\partial S}{\partial y(x_i)} = 0 \quad (24)$$

where  $(\partial/\partial y(x_j))$  implies differentiation with respect to  $y$  at every point  $x_j$ .

From equation (17) the second term of equation (24) is:

$$\frac{\partial S}{\partial y(x_j)} = \begin{cases} \frac{\partial S}{\partial y(X_i)} & \text{if } x_j = X_i \\ 0 & \text{if } x_j \neq X_i \end{cases} \quad (25)$$

or

$$\frac{\partial S}{\partial y(x_j)} = 2 \sum_{i=1}^m (y_i - Y_i) \cdot \delta_{ij} \quad (26)$$

where

$$\delta_{ij} = \begin{cases} 1 & \text{if } x_j = X_i \\ 0 & \text{if } x_j \neq X_i \end{cases}$$

Substituting equations (23) and (26) into equation (24) gives:

$$2/(\Delta x)^3 \cdot \downarrow \left( \overset{j' \rightarrow}{C_{jj}} \right) \cdot \downarrow \left( y_j \right) + 2\lambda \downarrow \left( \frac{(y_j - Y_i)}{\sigma_i^2} \delta_{ij} \right) = 0 \quad (27)$$

where  $i=1, \dots, m$  refers to the data values.

while  $j=1, \dots, n$  refers to the points  $y_j$  (or  $y(x_j)$ ) which describe the the smooth curve  $y(x)$ .

Next, various other values are assigned to the " $\lambda$ " parameter and equation (27) is solved for other sets of  $y(x_j)$ 's. For any given set of  $y(x_j)$ 's a measure of the deviation from the data points  $Y(X_i)$  can be computed from the equation:

$$S = \frac{\overbrace{y(X_i) - Y(X_i)}^L}{\sigma_i} \rightarrow \downarrow \left( \frac{y(X_i) - Y(X_i)}{\sigma_i} \right) \quad (28)$$

Therefore, the set of points  $y(x_j)$ , as determined for a given value of the " $\lambda$ " parameter, will be characterized by a value of the deviation term, "s", as computed by equation (28).

The following example illustrates the smoothing technique. Consider measurements of the electron density of the ionosphere vs. height as data values obtained from a vertically incident rocket. The problem is to "smooth out" the error in the data and interpolate between data points by drawing a smooth curve close to but not necessarily through the data points. The error in each measurement will be assumed to be gaussian with standard error,  $\sigma_i$ .

There are 20 heights at which data points are taken and these height values are 2 km apart. The height values for the computed smooth curve will be 1 km apart. To apply the procedure as presented by equations (14) through (28), let the height parameter be taken as the independent variable,  $x$ , and the log of the electron densities (i.e.  $\log_{10} N$ ) be taken as the dependent variable,  $y$ . The optimum value of the deviation parameter "s" is obtained when the fit between the data and the curve

$y(x) \equiv \log_{10} N(x)$  is, on the average, within one " $\sigma$ " value at each data point. That is, for 20 data points "s(optimum)" will be equal to 20.

Figures 5 through 9 illustrate the smoothing procedure as applied to the rocket experiment. Figure 5 shows what will be called the true electron density profile along with the "data" values which are obtained by adding random gaussian values to the true density values at each of the 20 heights.

Figure 6 presents the results obtained after applying the smoothing technique to the data (with gaussian error included). Shown are the resulting curve for "optimum smoothing" (i.e.  $s \approx 20$ ) and the curve for "over smoothing" (i.e.  $s = 31.1$ ). Over-smoothing implies that minimization of the curvature term, "c" of equation (14) is being accomplished at the expense of not fitting well to the data points. That is, the choice of  $\lambda$  is too small and needs to be increased.

Figure 7 compares the true profile with the optimally smoothed profile.

Figure 8 gives curves for "optimum smoothing" and for the case of "under-smoothing" (i.e.  $s = 9.1$ ). In the instance of "under-smoothing" the minimization of the term for deviation to the data points (i.e. "s") is dominant over minimizing the curvature term. The smooth curve  $y(x)$  is being attracted more strongly to the data points. This result implies that the choice of " $\lambda$ " is too large and should be decreased.

If the value of " $\lambda$ " is increased still further than that of figure 8, it is shown in figure 9 that the resulting smooth curve,  $y(x)$ , is a fit to the "error" rather than to the true profile. This result is an important aspect of the smoothing procedure when there is error in the data values.

## 2. Limiting Case of Interpolation Between Data Points.

Given a set of data points  $Y(X_i)$ , where  $i=1, \dots, m$ . Next consider the set of evenly spaced points  $x_j$ ,  $j=1, \dots, n$ , which include the set  $X_i$ . The problem is to find the values of terms  $y(x_j)$ , corresponding to the various  $x_j$ 's, by interpolation between the  $Y(X_i)$  values.

Consider equation (27), that is:

$$(\Delta X)^{-3} \downarrow \left( \overset{j'}{\overrightarrow{C_{j,j'}}} \right) \downarrow \left( \overset{j'}{y_j} \right) + \lambda \downarrow \left( \frac{(y_j - Y_i)}{\sigma_i^2} \overset{j'}{\delta_{i,j}} \right) = 0 \quad (27)$$

In the limit as " $\lambda$ "  $\rightarrow \infty$  equation (27) becomes:

$$\downarrow \left( \overset{j'}{\overrightarrow{C_{j,j'}}} \right) \overset{II-b}{\cdot} \downarrow \left( \overset{j'}{y_j} \right) = \downarrow \left( \overset{j'}{V_j} \right) \quad (29)$$

where:

$y_j = y(x_j)$ ,  $j=1, \dots, n$  are interpolated values at evenly spaced increments in  $x$  (i.e.  $\Delta x$ ) and which include the set of  $Y(X_i)$ 's.

$Y_i = Y(X_i)$ ,  $i = 1, \dots, m$  are data values at each  $X_i$ .

Note that each  $Y_i$  must be identical to a  $y_j$ . Also the modified  $C$  matrix is identified by the superscript II-b to differentiate it from other forms used in later sections of this report.

The  $j'$ -th row of the modified matrix,  $\overset{II-b}{C_{j',j}}$ , is the  $j'$ -th row of the matrix  $C_{j',j}$  (see equation (22)) if  $x_{j'}$  does not correspond to an  $X_i$ . If  $x_{j'}$  does correspond to an  $X_i$ , then the  $j'$ -th row of  $\overset{II-b}{C_{j',j}}$  is all

zeros except for a 1 for the main diagonal element,  $c_{j,j_1}$ . Also, all elements of the vector  $v_{j_1}$  of equation (29) are zero except that if  $x_{j_1}$  corresponds to an  $x_i$ , then  $v_{j_1} = y_i$ .

As an example, consider the set of points  $y_1, y_2$  and  $y_3$  at  $x_1, x_2$  and  $x_3$ . Now assume there are a set of  $x_j$ 's (separated by even increments) positioned between the  $x_i$ 's. Let there be 4  $x_j$  increments located between successive  $x_i$  values with two  $x_j$  increments preceding  $x_1$  and two increments of  $x_j$  following  $x_3$ . That is,  $x_3 \equiv x_1, x_7 \equiv x_2$ , and  $x_{11} \equiv x_3$ . When these assumptions are substituted into equation (29), the following matrix expression results.

$$\left( \begin{array}{ccccccccc}
 1 & -2 & 1 & 0 & & & & & \\
 -2 & 5 & -4 & 1 & 0 & & & & \\
 0 & 0 & 1 & 0 & 0 & & & & \\
 0 & 1 & -4 & 6 & -4 & 1 & 0 & & \\
 0 & 1 & -4 & 6 & -4 & 1 & 0 & & \\
 0 & 1 & -4 & 6 & -4 & 1 & 0 & & \\
 0 & 0 & 0 & 1 & 0 & 0 & 0 & & \\
 0 & 1 & -4 & 6 & -4 & 1 & 0 & & \\
 0 & 1 & -4 & 6 & -4 & 1 & 0 & & \\
 0 & 1 & -4 & 6 & -4 & 1 & 0 & & \\
 0 & 0 & 0 & 1 & 0 & 0 & 0 & & \\
 0 & 1 & -4 & 5 & -2 & & & & \\
 0 & 1 & -2 & 1 & & & & & \\
 \end{array} \right) \cdot \left( \begin{array}{c} y_1 \\ y_2 \\ y_3 \\ y_4 \\ y_5 \\ y_6 \\ y_7 \\ y_8 \\ y_9 \\ y_{10} \\ y_{11} \\ y_{12} \\ y_{13} \end{array} \right) = \left( \begin{array}{c} 0 \\ 0 \\ y_1 \\ 0 \\ 0 \\ 0 \\ y_2 \\ 0 \\ 0 \\ 0 \\ y_3 \\ 0 \\ 0 \end{array} \right) \quad (30)$$

The interpolated values,  $y_j$ , are then found from the matrix equation:

$$\downarrow \begin{pmatrix} y_j \\ \vdots \end{pmatrix} = \downarrow \begin{bmatrix} \xrightarrow{i} \\ \left( \begin{matrix} C_{ij} \\ \text{mod.} \end{matrix} \right)^{\pi-b} \end{bmatrix}^{-1} \cdot \downarrow \begin{pmatrix} V_j \\ \vdots \end{pmatrix} \quad (31)$$

It is shown in appendix C that the  $y_j$ 's, obtained by using this smoothing technique, are linear combinations of the  $Y_i$ 's. That is:

$$\downarrow \begin{pmatrix} y_j \\ \vdots \end{pmatrix} = \downarrow \begin{bmatrix} \xrightarrow{i} \\ b_{ji} \end{bmatrix} \downarrow \begin{pmatrix} Y_i \\ \vdots \end{pmatrix} \quad (32)$$

where

$$\downarrow \begin{bmatrix} \xrightarrow{i} \\ b_{ji} \end{bmatrix} = \downarrow \begin{bmatrix} \xrightarrow{i} \\ \left( \begin{matrix} C_{ij} \\ \text{mod.} \end{matrix} \right)^{\pi-b} \end{bmatrix}^{-1} \downarrow \begin{bmatrix} \xrightarrow{i} \\ V_{ji} \end{bmatrix} \quad (33)$$

and

$$(V_{ji}) = \begin{cases} 1 & \text{if } x_{j'} = X_i \\ 0 & \text{if } x_{j'} \neq X_i \end{cases} \quad (34)$$

It is also shown in appendix C that derivatives at the interpolation points,  $x_j$ , are given by:

$$\frac{dy}{dx_j} = \sum_{i=1}^m (\beta_{ji}) Y_i \quad (35)$$

$$j = 2, \dots, n-1$$

where

$$\beta_{jl} = \frac{1}{2\Delta x} (b_{j+1,l} - b_{j-1,l}) \quad (36)$$

### C. Combination Problem of Smoothing and Inversion

Define a function  $r(\omega)$  as:

$$r(\omega) = \int_a^b [K(\omega, \alpha(z), z) \cdot \alpha(z)] dz \quad (37)$$

So that the curve,  $r(\omega)$  is a function of the curve,  $\alpha(z)$ .

Now, suppose that at a finite number of values of  $\omega$  (i.e.  $\omega_i$ ,  $i=1, \dots, m$ ) there are data values,  $R(\omega_i) = R_{\text{true value}}(\omega_i) + \epsilon_i$ . See figure 10. The error,  $\epsilon_i$ , is unknown; however, the expected error is  $\sigma_i$ . From these data values,  $R(\omega_i)$ , it is desired to deduce the form of the curve,  $\alpha(z)$ , insofar as possible. The curve  $\alpha(z)$  can not be determined exactly because (a) there are only a finite number of data values,  $R(\omega_i)$  and (b) there is unknown error in the data. This problem is one of both smoothing and inversion.

Because of the error in the data,  $R(\omega_i)$ , it may not be desirable to represent  $\alpha(z)$  as a curve for which the  $r(\omega_i)$  fit the data values exactly. The optimum curve,  $\alpha(z)$ , should be one which contains all the detail justified by the data, but which does not contain spurious detail which would represent fitting to error in the data.

The trade-off between fit to data and smoothness of the curve may be represented by equation (14) as:

$$C + \lambda S \rightarrow \text{minimum} \quad (14)$$

where "c" is the measure of curvature in  $\alpha(z)$  and "s" is a measure of the deviation of values  $r(\omega_i)$ , on the curve  $r(\omega)$ , from the data values,  $R(\omega_i)$ .

The function "s" is defined as:

$$S = \underbrace{\frac{r(\omega_i) - R(\omega_i)}{\sigma_i}}_{\substack{\uparrow \\ L \rightarrow}} \cdot \underbrace{\sqrt{\left( \frac{r(\omega_i) - R(\omega_i)}{\sigma_i} \right)}}_{\substack{\downarrow \\ L}} \quad (38)$$

where the

$\sigma_i$ 's are the uncertainties in the data.

The function "c" is defined as:

$$C = \int_a^b \left\{ \frac{d^2 \alpha(z)}{dz^2} \right\}^2 dz \quad (39)$$

The parameter " $\lambda$ " of equation (14) is chosen so as to optimize the trade-off between the fit to the data  $R(\omega_j)$  and the smoothness of the curve  $\alpha(z)$ .

For the sake of numerical tractability, the curve  $\alpha(z)$  is represented by a series of short segments, see figure 11. The values of  $\alpha(z)$  where the segments join (i.e. at  $z_j$ ,  $j=1, \dots, n$ ) are taken to be the unknown parameters of  $\alpha(z)$  and are denoted by  $\alpha(z_j) = \alpha_j$ ,  $j=1, \dots, n$ .

Because  $\alpha(z)$  can only be determined at a finite number of points,  $z_j$ , and since for simplicity it will be assumed that the  $z_j$ 's are equally spaced at intervals  $\Delta z$ , the derivative in equation (39) at  $z_j$  is represented by:

$$\frac{d^2\alpha(z)}{dz^2} \sim \left[ \frac{(\alpha_{j-1} - \alpha_j)}{\Delta z} - \frac{(\alpha_j - \alpha_{j+1})}{\Delta z} \right] / \Delta z \quad (40)$$

As given previously in equation (20), the curvature function, "c" can then be approximated by:

$$c \sim \left[ \sum_{j=2}^{n-1} (\alpha_{j-1} - 2\alpha_j + \alpha_{j+1})^2 \right] / (\Delta z)^3 \quad (41)$$

where  $n$  is the number of segment points,  $z_j$ .

Equation (41) can be written in matrix notation as:

$$c \sim (\Delta z)^{-3} \underbrace{\alpha_j}_{\substack{\xrightarrow{j} \\ \alpha_j}} \cdot \underbrace{\begin{pmatrix} \xrightarrow{j} \\ C_{j,j} \\ \downarrow \end{pmatrix}}_{\substack{\xrightarrow{j} \\ C_{j,j} \\ \downarrow}} \cdot \underbrace{\begin{pmatrix} \xrightarrow{j} \\ \alpha_j \\ \downarrow \end{pmatrix}}_{\substack{\xrightarrow{j} \\ \alpha_j \\ \downarrow}} \quad (42)$$

where the matrix  $C_{j,j}$  is given in equation (22).

The minimization of equation (14) is with respect to the positions of the points  $\alpha(z_j)$  on the curve  $\alpha(z)$ . Therefore, the minimization condition is met if:

$$\frac{\partial C}{\partial \alpha(z_j)} + \lambda \frac{\partial S}{\partial \alpha(z_j)} = 0 \quad (43)$$

where  $j=1, \dots, n$

The derivative  $(\partial C / \partial \alpha(z_j))$  is given by:

$$\downarrow \overset{i}{\overset{\rightarrow}{\left( \frac{\partial C}{\partial \alpha_j} \right)}} = \frac{2}{(\Delta z)^3} \downarrow \overset{i}{\overset{\rightarrow}{\left( C_{j,j} \right)}} \cdot \downarrow \overset{i}{\overset{\rightarrow}{\left( \alpha_j \right)}} \quad (44)$$

which is similar to equation (23).

The derivative  $(\partial S / \partial \alpha(z_j))$  is given by:

$$\downarrow \overset{i}{\overset{\rightarrow}{\left( \frac{\partial S}{\partial \alpha_j} \right)}} = 2 \cdot \downarrow \overset{i}{\overset{\rightarrow}{\left[ \frac{\partial r_i}{\partial \alpha_j} \right]}} \cdot \downarrow \overset{i}{\overset{\rightarrow}{\left( \frac{r_i - R_i}{\sigma_i} \right)}} \quad (45)$$

where  $r_i = r(\omega_i)$ , ( $i=1 \dots m$ ) is computed from equation (37) using the values  $\alpha_j = \alpha(z_j)$ . For purposes of integration, linear interpolation is made between the points  $\alpha(z_j)$ .

The derivative,  $(\partial r_i / \partial \alpha_j)$ , is given by:

$$\frac{\partial r_i}{\partial \alpha_j} = \frac{\partial r(\omega_i)}{\partial \alpha(z_j)} = \int_a^b \left\{ \frac{\partial K(\omega_i, \alpha(z), z)}{\partial \alpha(z_j)} \cdot \alpha(z) \right. \\ \left. + K(\omega_i, \alpha(z), z) \right\} \cdot \frac{\partial \alpha(z)}{\partial \alpha(z_j)} dz \quad (46)$$

where  $(\partial \alpha(z) / \partial \alpha(z_j))$  is a triangular weighting function made necessary by the use of linear interpolation in the integration and is given by:

$$\frac{\partial \alpha(z)}{\partial \alpha(z_j)} = \frac{\partial \alpha}{\partial \alpha_j} = \begin{cases} \left( \frac{z_{jH} - z}{z_{jH} - z_j} \right) & \text{if } z_j \leq z < z_{j+1} \\ \left( \frac{z - z_{j-1}}{z_j - z_{j-1}} \right) & \text{if } z_{j-1} < z \leq z_j \\ 0 & \text{otherwise} \end{cases} \quad (47)$$

See figure 12, where the ratio  $(\partial \alpha / \partial \alpha_j)$  is:

$$\frac{\Delta \alpha}{\Delta \alpha_j} = \left( \frac{z - z_{j-1}}{z_j - z_{j-1}} \right)$$

Substituting equations (44) and (45) into equation (43) gives:

$$\frac{1}{(\Delta z)^3} \downarrow^i \left( \overset{j \rightarrow}{\downarrow^j} \left( C_{jj} \right) \cdot \downarrow^j (\alpha_j) \right) + \lambda \cdot \downarrow^i \left[ \overset{i \rightarrow}{\downarrow^i} \left( \frac{\partial r_i}{\partial \alpha_j} \right) \right] \cdot \downarrow^i \left( \frac{r_i - R_i}{\sigma_i^2} \right) = \downarrow^i (0) \quad (48)$$

where  $r_i = r(\omega_i)$  and is given by equation (37). Also, the rectangular matrix  $(\partial r_i / \partial \alpha_j)$  is given by equations (46) and (47).

Note that the unknowns in equation (48) are the  $\alpha_j$ 's but that the  $r_i$ 's are functions of these "unknown"  $\alpha_j$ 's. Hence, at this point equation (48) cannot be used to solve for the  $\alpha(z)$  curve.

With certain additional constraints in the curve,  $\alpha(z)$ , the equation may, however, be solved for " $\lambda$ " = 0, for which values of  $r(\omega_i)$  are not required. Without additional constraints the solution for " $\lambda$ " = 0 is indeterminate since any straight line form of  $\alpha(z)$  is a solution. That is, for any straight line, the curvature function "c" = 0. The required additional constraints could be, for example, that the values  $\alpha(a) = \alpha_1$  and  $\alpha(b) = \alpha_n$  be pre-selected fixed values. These constraints may be added by modifying certain elements of the  $C$  matrix of equation (22).

That is by setting:

$$C_{12} = C_{13} = C_{n,n-2} = C_{n,n-1} = 0 \quad (49)$$

and by setting the first element of the right-hand vector of equation (48) to  $\alpha(a)$  and the last element to  $\alpha(b)$ . If these constraints are retained for other values of " $\lambda$ " as well, equation (48) becomes:

$$\downarrow \left( \begin{array}{c} \overset{i}{\rightarrow} \\ C_{ij} \\ \downarrow \\ \text{mod.} \end{array} \right) \overset{\text{II}-c}{\rightarrow} \downarrow \left( \begin{array}{c} \alpha_j \\ \downarrow \end{array} \right) + \lambda \downarrow \left( \begin{array}{c} \overset{i}{\rightarrow} \\ \frac{\partial r_i}{\partial \alpha_j} \\ \downarrow \end{array} \right) \downarrow \left( \begin{array}{c} r_i - R_i \\ \sigma_i^{-2} \end{array} \right) = \downarrow \left( \begin{array}{c} V_i \\ \downarrow \end{array} \right) \quad (50)$$

where the modified C matrix,  $C^{II-C}$  contains the changes just described and contains the factor  $(1/\Delta x^3)$ . Also, for this case the vector "V" is

$$\downarrow \begin{pmatrix} V_j \\ \vdots \\ V_j \end{pmatrix} = \downarrow \begin{pmatrix} \alpha^{(a)} \\ 0 \\ \vdots \\ 0 \\ \alpha^{(b)} \end{pmatrix} \quad (51)$$

Note that other constraints are, of course, possible.

The solution to equation (50) for " $\lambda$ " = 0 is a set of  $\alpha_j$ 's representing a straight line between the fixed points  $\alpha(a)$  and  $\alpha(b)$ . Although exact solutions to equation (50) may not be obtained for other values of " $\lambda$ ", a first-order solution may be found for a small positive value of " $\lambda$ " if  $r_i$  is approximated by a first order Taylor expression:

$$\downarrow \begin{pmatrix} r_i \\ \vdots \\ r_i \end{pmatrix} = \downarrow \begin{pmatrix} r_i^0 \\ \vdots \\ r_i^0 \end{pmatrix} + \downarrow \begin{pmatrix} \frac{\partial r_i}{\partial \alpha_j} \end{pmatrix} \cdot \downarrow \begin{pmatrix} \alpha_j - \alpha_j^0 \\ \vdots \\ \alpha_j - \alpha_j^0 \end{pmatrix} \quad (52)$$

where  $\alpha_j^0$  refers to the solution for  $\lambda = 0$  and  $r_i^0$  and  $(\partial r_i / \partial \alpha_j)_0$  are values obtained from equations (37) and (46) respectively. Equation (50) is then approximated by:

$$\downarrow \begin{pmatrix} \frac{\partial \mathbf{C}_{ij}}{\partial \alpha_j} \\ \vdots \\ \frac{\partial \mathbf{C}_{ij}}{\partial \alpha_j} \end{pmatrix} \cdot \downarrow \begin{pmatrix} \alpha_j \\ \vdots \\ \alpha_j \end{pmatrix} + \lambda \downarrow \begin{pmatrix} \frac{\partial r_i}{\partial \alpha_j} \\ \vdots \\ \frac{\partial r_i}{\partial \alpha_j} \end{pmatrix} \cdot \downarrow \begin{pmatrix} \alpha_j - \alpha_j^0 \\ \vdots \\ \alpha_j - \alpha_j^0 \end{pmatrix} \quad (53)$$

$$\cdot \left\{ \downarrow \begin{pmatrix} r_i^0 \\ \vdots \\ r_i^0 \end{pmatrix} + \downarrow \begin{pmatrix} \frac{\partial r_i}{\partial \alpha_j} \end{pmatrix} \cdot \downarrow \begin{pmatrix} \alpha_j - \alpha_j^0 \\ \vdots \\ \alpha_j - \alpha_j^0 \end{pmatrix} - \downarrow \begin{pmatrix} r_i \\ \vdots \\ r_i \end{pmatrix} \right\} = \downarrow \begin{pmatrix} V_j \\ \vdots \\ V_j \end{pmatrix}$$

If  $\Delta \alpha_j$  is defined as  $(\alpha_j - \alpha_j^0)$ , equation (53) may be written

$$\begin{aligned}
 & \left\{ \underset{\text{mod.}}{\downarrow} \left( \underset{i}{\overset{i \rightarrow}{\mathcal{L}}} \right) \underset{i}{\overset{i \rightarrow}{\mathcal{L}}} + \lambda \underset{i}{\downarrow} \left[ \frac{\partial r_i}{\partial \alpha_j} \right] \cdot \underset{i}{\downarrow} \left( \frac{1}{\sigma_i^2} \right) \cdot \underset{i}{\downarrow} \left[ \frac{\partial r_i}{\partial \alpha_j} \right] \right\} \cdot \underset{i}{\downarrow} (\Delta \alpha_j) \quad (54) \\
 & = - \left\{ \underset{\text{mod.}}{\downarrow} \left( \underset{i}{\overset{i \rightarrow}{\mathcal{L}}} \right) \cdot \underset{i}{\downarrow} (\alpha_j^0) - \underset{i}{\downarrow} (V_i) + \lambda \underset{i}{\downarrow} \left[ \frac{\partial r_i}{\partial \alpha_j} \right] \cdot \underset{i}{\downarrow} \left( \frac{1}{\sigma_i^2} \right) \cdot \underset{i}{\downarrow} (r_i^0 - R_i) \right\}
 \end{aligned}$$

In this matrix equation only the  $\Delta \alpha_j$ 's are not known and hence the equation may be used to solve for  $\Delta \alpha_j$ . Then:

$$\alpha(z_j) = \alpha^0(z_j) + \Delta \alpha_j \quad ; \quad j = 1, \dots, n \quad (55)$$

is an approximate solution for the small value of " $\lambda$ " used in the equation.

If the  $\alpha_j^0$  values in equation (54) are now taken to be the values just found for small " $\lambda$ ", this equation may be used with a somewhat larger value of " $\lambda$ " to obtain a new curve,  $\alpha(z)$ , represented by values,  $\alpha_j$ . Thus, as long as the increments in " $\lambda$ " are sufficiently small and so long as the coefficient matrix does not become singular, equation (54) may be used in "bootstrap" fashion to obtain values of  $\alpha_j$  for any value of " $\lambda$ ". That is, for a given value of " $\lambda$ ", equation (54) is solved for  $(\Delta \alpha_j)$ . Then  $\alpha_j$  (new) is computed from equation (55) as  $\alpha_j$  (new) =  $\alpha_j$  (old) +  $\Delta \alpha_j$ . At this point new values of  $r_i$  and  $(\partial r_i / \partial \alpha_j)$  are computed. The next step is to substitute these "new" values into equation (54), along with a new

value of " $\lambda$ " and then to solve the equation for yet another set of  $(\Delta\alpha_j)$ .

Equation (54) may also be written in a simplified form as:

$$[\underline{\underline{K}}] \cdot \overrightarrow{(\Delta\alpha_j)} = \overrightarrow{(\bar{T})} \quad (56)$$

where  $[\underline{\underline{K}}]$  is the coefficient matrix,

$\overrightarrow{(\Delta\alpha_j)}$  is the unknown vector

and  $\overrightarrow{(\bar{T})}$  is a known vector.

The solution for  $(\Delta\alpha_j)$  is found from:

$$\overrightarrow{(\Delta\alpha_j)} = [\underline{\underline{K}}]^{-1} \cdot \overrightarrow{(\bar{T})} \quad (57)$$

It may be noted that equation (57) is similar in form to equation (12).

In section A it was shown that the modified Newton-Raphson procedure diverged if the derivative of  $f(x)$  became zero anywhere along the  $f(x)$  curve being followed. That is where:

$$\Delta X = \left( \frac{df(x)}{dx} \right)^{-1} \Big|_{x=x_i} \cdot \Delta F \quad (58)$$

and

$$\left( \frac{df(x)}{dx} \right) = 0 \quad (59)$$

An analogy exists between equation (57) and equation (58) in that the procedure for solving equation (57) will also diverge if the coefficient matrix,  $K$ , becomes singular.

Also, in analogy with section A, if divergence occurs, there may be another function,  $g(\omega) = \text{function } (r(\omega))$ , which may be followed to the desired inverse solution without a singularity being encountered. The choice of function,  $g(\omega)$ , however, is likely to be an art more than a science, unless sufficient information is available on the behavior of these functions.

The matrix equation to be used with  $g(\omega) = \text{function } (r(\omega))$  is simply equation (54) with the  $r_i$ 's replaced by  $g_i$ 's and the appropriate choice made for the matrix of uncertainties,  $\sigma_i$ . These "uncertainties" are probably best determined by requiring that as " $\lambda$ " is increased to make the values of  $g_i$  approach the values  $G_i = \text{function } (R_i)$ , the sequence of curves,  $\alpha(z)$ , become the same as if the function  $r(\omega)$  were used. The formulation needed for making such a choice of "uncertainties" in  $G(\omega_i)$  is given in appendix D, where it is seen that the uncertainty matrix for the  $G_i$ 's is no longer diagonal. For the  $g_i$ 's equation (54) becomes:

$$\left\{ \begin{matrix} \downarrow \left( \begin{matrix} \overset{i \rightarrow}{C_{ij}} \\ \text{med} \end{matrix} \right) + \lambda \downarrow \left[ \frac{\partial g_i}{\partial \alpha_j} \right] \downarrow \left( \begin{matrix} \overset{i \rightarrow}{\frac{1}{\sigma_{ii}}} \\ \end{matrix} \right) \downarrow \left( \begin{matrix} \overset{i \rightarrow}{\frac{1}{\sigma_{ii}}} \\ \end{matrix} \right) \downarrow \left[ \frac{\partial g_i}{\partial \alpha_j} \right] \\ \end{matrix} \right\} \downarrow \left( \begin{matrix} \overset{i \rightarrow}{\Delta \alpha_j} \\ \end{matrix} \right) \quad (60)$$

$$= - \left[ \begin{matrix} \downarrow \left( \begin{matrix} \overset{i \rightarrow}{C_{ij}} \\ \text{med} \end{matrix} \right) \cdot \downarrow \left( \begin{matrix} \overset{i \rightarrow}{\alpha_j} \\ \end{matrix} \right) - \downarrow \left( \begin{matrix} \overset{i \rightarrow}{V_j} \\ \end{matrix} \right) + \lambda \downarrow \left[ \begin{matrix} \overset{i \rightarrow}{\frac{\partial g_i}{\partial \alpha_j}} \\ \end{matrix} \right] \cdot \downarrow \left( \begin{matrix} \overset{i \rightarrow}{\frac{1}{\sigma_{ii}}} \\ \end{matrix} \right) \cdot \downarrow \left( \begin{matrix} \overset{i \rightarrow}{\frac{1}{\sigma_{ii}}} \\ \end{matrix} \right) \cdot \downarrow \left( \begin{matrix} \overset{i \rightarrow}{g_i - G_i} \\ \end{matrix} \right) \end{matrix} \right]$$

where:

$$S = \underbrace{\downarrow \left( \begin{matrix} \overset{i \rightarrow}{g_i - G_i} \\ \end{matrix} \right)}_{\text{S}} \cdot \downarrow \left( \begin{matrix} \overset{i \rightarrow}{\frac{1}{\sigma_{ii}}} \\ \end{matrix} \right) \cdot \downarrow \left( \begin{matrix} \overset{i \rightarrow}{\frac{1}{\sigma_{ii}}} \\ \end{matrix} \right) \cdot \downarrow \left( \begin{matrix} \overset{i \rightarrow}{g_i - G_i} \\ \end{matrix} \right) \quad (61)$$

### III. DETERMINATION OF ELECTRON DENSITY PROFILES FROM VLF REFLECTION COEFFICIENTS

#### A. Reflection Coefficient Data

Very low frequency (VLF) reflection coefficient data may be obtained from steep-incidence sounders, such as the NOSC facility located at Sentinel, Arizona, reference 6. This system uses a horizontal dipole as a transmitting antenna and crossed loops for receiving. The system has the ability to transmit several frequencies nearly simultaneously.

Reflection of a VLF wave at near-vertical incidence is described by the reflection matrix:

$$\tilde{R} = \begin{pmatrix} \parallel R_{\parallel} & \perp R_{\parallel} \\ \parallel R_{\perp} & \perp R_{\perp} \end{pmatrix} \quad (62)$$

where the first subscript refers to the polarization of the upgoing wave with respect to the plane of incidence, and the second subscript refers to the polarization of the downcoming wave.

The measured parameters of the sounding system consist of the received electric fields, both parallel and perpendicular to the plane of incidence, of the VLF radio wave. These fields are identified as  $E_{\parallel}$  and  $E_{\perp}$  respectively.

The transmitted wave,  $E_T$ , is used to form the ratios:

$$\left\{ \begin{array}{l} \perp R_{\perp} = \frac{E_{\perp}}{E_T} \\ \perp R_{\parallel} = \frac{E_{\parallel}}{E_T} \end{array} \right\} \quad (63)$$

These ratios are combined to give:

$$\frac{\perp R_{\parallel}}{\perp R_{\perp}} = \frac{E_{\parallel}/E_T}{E_{\perp}/E_T} = \frac{E_{\parallel}}{E_{\perp}} \quad (64)$$

thus eliminating the need for knowing the transmitted wave,  $E_T$ .

The ratio term,  $(\perp R_{\parallel}/\perp R_{\perp})$ , has the property that, for some forms of the ionosphere, the magnitude of the denominator may become much smaller than the magnitude of the numerator. This gives a very large value for the ratio. The same result is also characteristic of the reciprocal of this ratio. The large value constitutes a major numerical disadvantage of using this type of ratio in the electron density profile determination scheme described in a later section of this report.

Following Budden, reference 7, a better choice of parameter is:

$$r = \left[ \frac{-1 + j(\perp R_{\parallel}/\perp R_{\perp})}{-1 - j(\perp R_{\parallel}/\perp R_{\perp})} \right] \quad (65)$$

where  $j = \sqrt{-1}$

This ratio is derived for the case of vertical incidence propagation through an exponential electron density profile with a constant collision frequency and assuming the earth's magnetic field to be vertical. This ratio has the characteristic that its magnitude is always less than or equal to one for the case for which it was derived. For the general case, however, it will also give results that are not so large as to give numerical problems when used in the profile determination scheme, for latitudes not too near the equator.

Equation (65) may also be re-written in the form:

$$R(\omega_i) = \left\{ \frac{-_1 R_{\perp}(\theta) + j \perp R_{\parallel}(\theta)}{-_1 R_{\perp}(\theta) - j \perp R_{\parallel}(\theta)} \right\}_i \quad (66)$$

where  $i = 1, \dots, m$

In this case the terms are identified as:

$\omega_i$  = The transmitted frequency.

$m$  = The total number of transmitted frequencies.

$R(\omega_i)$  = The value of the ratio, at the  $i$ -th transmitted frequency, as determined from data.

$\theta$  = The incident angle of the radio wave on to the ionosphere.

$j = \sqrt{-1}$

It is to be noted that the above reflection coefficients are functions of the earth's magnetic field. In particular, as the location of the sounder site approaches the geomagnetic equator, the cross term (i.e.  $\perp R_{\parallel}$ ) tends to zero and the ratio term,  $R(\omega_i)$  becomes equal to one. When this situation occurs the profile determination technique then yields no information. The most useful data for determining profiles is obtained, therefore, at locations with large magnetic dip angles (i.e. near the geomagnetic poles).

In equation (66) all of the reflection coefficient terms imply complex numbers. Also, the ratio term,  $R(\omega_i)$  is a complex number. A useful representation of the reflection coefficient data is to plot it in the complex  $R$ -plane as a function of the data frequencies,  $\omega_i$ . An example of this relationship is illustrated in figure 13 for the real and imaginary components of  $R(\omega_i)$ . Note that the frequency,  $\omega$ , serves as the parametric variable.

Included in figure 13 is a smooth curve which would represent the data if it were obtained at all frequencies without experimental error.

## B. The Ionospheric Model

It is proposed to investigate the possibility that the form of the electron density profile of the ionosphere can be deduced from steep incidence sounder measurements of reflection coefficients (equation (62)), since the measured values depend on the height variation of electron density. These values also depend on the charge, and mass of the particles in the ionosphere, as well as their collision frequencies with neutral particles and of the earth's magnetic field.

Several assumptions about the electron density vs. height relationship in the ionosphere must be made before a mathematical technique can be set up to determine a profile from reflection coefficient data. In particular, all of the above parameters will be taken as known except the electron density profile which will be considered as unknown and is to be found from the data.

The magnetic-field parameters will be taken to be known and, in the case of the model presented here, the magnetic azimuth will be restricted to be either  $90^\circ$  or  $270^\circ$ . As is the usual case of these VLF frequencies, ions are considered to have negligible effect on propagation and hence are omitted from the model. The collision frequency profile is taken to be known and is constrained to be of exponential form (e.g.  $\nu = \nu_0 \text{ Exp}(-\alpha z)$ ).

Additional assumptions (i.e. constraints) on the form of the desired electron density profile are listed below and are illustrated in figure 14 where the electron density ( $N_e$ ) is shown as a function of ionospheric height in terms of  $\log_{10} N_e$ .

1. "Stop" constraints are introduced at both the top and bottom of the electron density profile. These correspond to limiting values of electron density which the profile may assume at these heights. At the top of the profile the "stop" defines the minimum value of

electron density which the profile may assume. At the bottom, the "stop" defines the maximum value for that height.

2. It is assumed that there are no electrons below the chosen lowest height of the profile. Above the chosen top height of the profile the electron density is assumed to be of constant value equal to the electron density at the chosen top height. This latter property is usually referred to as a semi-infinite medium.
3. The profile is constrained to be reasonably smooth but otherwise consistent with the reflection coefficient data. Note that this implies that the profile approaches a slope of  $(dN/dz) = 0$  near the top height which is just below the semi-infinite medium.

#### C. Computation of Ionospheric Reflection Coefficients

Ionospheric reflection coefficients,  $\tilde{R}$ , may be obtained for a given electron density profile by the "full-wave" method given in reference 4. These reflection coefficients are the result of the integration:

$$\tilde{R} = \int_a^b \left( \frac{d\tilde{R}}{dz} \right) dz \quad (67)$$

where the integrand is given in reference 4 as:

$$d\tilde{R}/dz = ik/2 \left\{ \mathcal{S}^{(21)} + \mathcal{S}^{(22)} \tilde{R} - \tilde{R} \mathcal{S}^{(11)} - \tilde{R} \mathcal{S}^{(12)} \tilde{R} \right\} \quad (68)$$

$k$  is the wave number.

The matrices, " $\mathcal{S}$ ", are functions of the electron density profile and of the wave frequency,  $\omega$ , as well as other parameters described in section B.

Equation (68) is given in scalar form in reference 5, pages 11 and 12.

As was discussed in section A, a useful function of the reflection coefficients is:

$$r(\omega_i) = \left\{ \frac{-\perp R_{\perp} + i \perp R_{\parallel}}{-\perp R_{\perp} - i \perp R_{\parallel}} \right\} \quad (69)$$

where  $i = 1, \dots, m$

with  $m$  being the total number of data frequencies.

In this instance the reflection coefficients,  $\perp R_{\perp}$  and  $\perp R_{\parallel}$ , are obtained from the integration in equation (67) and thus, " $r(\omega_i)$ " is the computed value of the ratio at the  $i$ -th data frequency.

The function " $r(\omega_i)$ " is complex and as such can be plotted in the complex  $r$ -plane as a function of its real and imaginary parts. Examples of  $r(\omega)$  curves are illustrated in figure 15 as a continuous function of the parametric variable,  $\omega$ . Calculations performed using different electron density profiles will produce various forms of the  $r(\omega)$  curve. Some of  $r(\omega)$  curves will possess certain distinct characteristics, such as the loop shown in figure 15 for the curve  $[r(\omega)]_1$ ; others may be relatively smooth, like the  $[r(\omega)]_2$  curve. Note that because of the constraints listed in part B, not all forms of the  $r(\omega)$  curve can be generated simply by varying the electron density profile.

#### D. Comparison of Data with Computed Reflection Coefficients

Reflection coefficient data may also be plotted in the complex  $R$ -plane. An example was presented in figure 13 where the data points were plotted parametric with frequency. If ionospheric reflection coefficients are computed from an assumed electron density profile, a plot illustrating the comparison between data and theoretical calculations may be constructed. Figure 16 shows an example of such a comparison. In this instance it is observed from

the plot that the computed reflection coefficients differ drastically from the data values. The problem to be solved, then, is to find that electron density profile which, when used in the full-wave computation of reflection coefficients, will produce a match to the data,  $R(\omega_j)$ . Such a match is illustrated in figure 17. Because of error in the data and because of the constraints put on the ionospheric model, the data can not be matched exactly. This characteristic is shown in figure 17.

The procedure for finding that particular profile of electron density which will produce a match to the data is discussed in the following sections of this report.

E. Application of the Combined Smoothing and Inversion Techniques to the Ionosphere Problem

The question as to whether the profile of the electron density of the ionosphere can be determined from reflection coefficient data is examined with reference to the procedure presented in section II, part C of this report.

The correspondence between certain variables may be identified. In particular, the following relations apply:

Section III

- a Height,  $z$  ~ The integration variable,  $z$
- b Wave frequency,  $\omega$  ~ Parametric variable,  $\omega$
- c  $\log N_e$  vs. height,  $z$  ~  $\alpha$  vs.  $z$
- d  $\log N_e$  at height,  $z_j$  ~  $\alpha_j = \alpha(z_j)$
- e  $\text{Re}[r(\omega)]$  &  $\text{Im}[r(\omega)]$  ~  $r(\omega)$
- f  $\text{Re}[r(\omega_j)]$  &  $\text{Im}[r(\omega_j)]$  ~  $r_j = r(\omega_j)$
- g  $\text{Re}[R(\omega_j)]$  &  $\text{Im}[R(\omega_j)]$  ~  $R_j = R(\omega_j)$

Section II,C

Note that the ionosphere  $r(\omega)$  is not obtained from an integration of exactly the form given in equation (37). However, the integration (67) together with equation (69) is comparable with the integration in equation (37)

in that the  $r(\omega)$  values are obtained as a result of an integration between fixed limits in the integration variable,  $z$ , and furthermore the integrand is a function of  $z, \alpha(z)$ , and  $\omega$ .

The derivative  $(\partial r / \partial \alpha_j)$  required in equation (54) of section II-C will correspondingly be somewhat different in form. It is first noted that:

$$\frac{\partial r}{\partial \alpha_j} = 2 \cdot J \cdot \left\{ \frac{\perp R_{||} \left( \frac{\partial \perp R_{||}}{\partial \alpha_j} \right) - \perp R_{||} \left( \frac{\partial \perp R_{||}}{\partial \alpha_j} \right)}{\left( -\perp R_{||} - J \perp R_{||} \right)^2} \right\}; \{J = \sqrt{-1}\} \quad (70)$$

the derivatives  $(\partial \perp R_{||} / \partial \alpha_j)$  and  $(\partial \perp R_{||} / \partial \alpha_j)$  are elements of the matrix

$$\frac{\partial \tilde{R}}{\partial \alpha_j} = \begin{pmatrix} \frac{\partial_{||} R_{||}}{\partial \alpha_j} & \frac{\partial_{\perp} R_{||}}{\partial \alpha_j} \\ \frac{\partial_{||} R_{\perp}}{\partial \alpha_j} & \frac{\partial_{\perp} R_{\perp}}{\partial \alpha_j} \end{pmatrix} \quad (71)$$

which is found as the result of the integration

$$\frac{\partial \tilde{R}}{\partial \alpha_j} = \int_a^b \frac{\partial}{\partial \alpha_j} \left( \frac{\partial \tilde{R}}{\partial z} \right) dz \quad (72)$$

The integrand is found by differentiating equation (68) with respect to  $\alpha_j$ :

$$\frac{\partial}{\partial \alpha_j} \left( \frac{dR}{dz} \right) = \frac{-jk}{2} \left\{ \left[ \frac{dS^{(21)}}{d\alpha} + \frac{dS^{(22)}}{d\alpha} R \cdot R \frac{dS^{(11)}}{d\alpha} \cdot R \frac{dS^{(12)}}{d\alpha} R \right] \frac{\partial \alpha}{\partial \alpha_j} \right. \\ \left. + \left[ S^{(22)} \frac{\partial R}{\partial \alpha_j} \cdot \frac{\partial R}{\partial \alpha_j} S^{(11)} \cdot \frac{\partial R}{\partial \alpha_j} S^{(12)} R \cdot R S^{(12)} \frac{\partial R}{\partial \alpha_j} \right] \right\} \quad (73)$$

$$\mathcal{J} = \sqrt{-1}$$

where the weighting factor  $(\partial \alpha / \partial \alpha_j)$  is described by equation (47). The derivatives  $(\partial "S" / \partial \alpha)$  are described in reference 5, pages 31-35.

The constraints on the  $\alpha(z)$  curve when it is used to represent the electron density profile are somewhat different than the ones placed on the  $\alpha(z)$  curve in section II-C. Instead of choosing the ends of the  $\alpha(z)$  curve (the profile) to be fixed values, inequalities are used. At the top of the profile the electron density is constrained to be at least as great as a chosen fixed value. At the bottom height of the profile, the electron density is constrained to be no greater than a chosen fixed value. Thus:

$$\alpha(a) = \alpha(z_1) > \alpha_{TOP\ STOP} \\ \alpha(b) = \alpha(z_n) < \alpha_{BOT.\ STOP} \quad (74)$$

In addition, in order to ensure a continuous slope,  $(dN_e/dz)$ , leading upward to the semi-infinite medium, the slope at the top of the profile

$(z = a = z_1)$  is constrained to approach that of the semi-infinite medium.

In terms of a segmented  $\alpha(z)$  curve, that is, a segmented electron density profile, this is implemented by adding the term:

$$(\alpha_2 - \alpha_1)^2 \cdot (\Delta z)^{-3} \quad (75)$$

to the summation representing the curvature function. That is, "c" is now defined as:

$$C = \left\{ (\alpha_2 - \alpha_1)^2 + \sum_{j=2}^{n-1} (\alpha_{j-1} - 2\alpha_j + \alpha_{j+1})^2 \right\} (\Delta z)^{-3} \quad (76)$$

Compare this result to equation (20).

With these modifications to the set of constraints, the equation to be solved is a modified form of equation (54). In particular the matrix:

$$\begin{pmatrix} (1 + P_T) & -1 & 0 & \cdots & 0 \\ -1 & +1 & 0 & \cdots & 0 \\ 0 & 0 & 0 & \cdots & 0 \\ \vdots & \vdots & \vdots & \ddots & \vdots \\ 0 & 0 & 0 & \cdots & P_B \end{pmatrix} \quad (77)$$

is added to the unmodified  $\underline{C}$  matrix of equation (22). That is, the original  $\underline{C}$  matrix terms are modified to be:

$$\left\{ \begin{array}{l} C_{11} = 1 + (1 + P_T) = 2 + P_T \\ C_{12} = -2 + (-1) = -3 \\ C_{21} = -2 + (-1) = -3 \\ C_{22} = 5 + (1) = 6 \\ C_{nn} = 1 + (P_B) = 1 + P_B \end{array} \right\} \quad (78)$$

Here:

(a)  $p_T$   $\begin{cases} = 0 \text{ if, in the solution for } \Delta\alpha_j \text{'s the top end of the profile} \\ \text{is inclined to move to the right of the stop.} \\ = \text{a very large positive value if the top end of the profile} \\ \text{is inclined to move to the left of the stop.} \end{cases}$

(b)  $p_B$   $\begin{cases} = 0 \text{ if, in the solution for } \Delta\alpha_j \text{'s, the bottom end of the} \\ \text{profile is inclined to move to the left of the stop.} \\ = \text{a very large value if the bottom end of the profile is} \\ \text{inclined to move to the right of the stop.} \end{cases}$

Also, the vector,  $\vec{V}_i$ , of equation (51), used in equation (54), is modified to be

$$\vec{V}_i = \begin{cases} \vec{P}_T \cdot \alpha_{top \ stop} \\ \vec{P}_B \cdot \alpha_{bot \ stop} \end{cases} \quad (79)$$

Substitution of equations (78) and (79) into equation (54) gives:

$$\begin{aligned} & \left\{ \vec{V}_i \cdot \left[ \frac{\partial r_i}{\partial \alpha_j} \right] \cdot \left[ \frac{\partial \alpha_j}{\partial \Delta \alpha_j} \right] \cdot \vec{V}_i \cdot \left[ \frac{\partial r_i}{\partial \Delta \alpha_j} \right] \right\} \cdot \vec{V}_i \cdot \left( \Delta \alpha_j \right) \\ & = - \left\{ \vec{V}_i \cdot \left[ \frac{\partial r_i}{\partial \alpha_j} \right] \cdot \vec{V}_i \cdot \left[ \frac{\partial r_i}{\partial \Delta \alpha_j} \right] \cdot \vec{V}_i \cdot \left[ \frac{\partial r_i}{\partial \Delta \alpha_j} \right] \cdot \vec{V}_i \cdot \left[ \frac{\partial r_i}{\partial \Delta \alpha_j} \right] \right\} \quad (80) \end{aligned}$$

where the  $r_i$ 's are the computed ionospheric reflection coefficient ratios as given by equation (69), the  $R_i$ 's are the data parameters given by

equation (66) and the  $\alpha_j$ 's are the logs of the electron densities at the profile segment points,  $z_j$ .

The derivatives,  $(\partial r_i / \partial \alpha_j)$ , are given by equations (70-73).

F. Characteristics of the Solution of Equations in Terms of the "r( $\omega$ )" Parameter

The solution to equations of the form of equation (80) was discussed previously in section II,C with regard to equation (54). The solution for successive iterative steps of  $\lambda + \Delta\lambda$  is given in terms of  $(\Delta\alpha_j)$ . Each iterative step leads to a new set of  $\alpha_j$ 's given by:

$$\alpha(z_j)_{\text{new}} = \alpha(z_j)_{\text{previous}} + (\Delta\alpha_j) \quad (81)$$

The procedure is to compute new sets of the ionospheric parameters,  $r(\omega)$ , from each set of  $\alpha(z_j)_{\text{new}}$ .

In section D the comparison of computed values,  $r(\omega_i)$ , and data values,  $R(\omega_i)$ , were shown plotted in the complex  $r$ -plane. The  $\omega_i$ 's are the propagation frequencies and serve as the parametric variable in the plots.

It was suggested that the proper choice of electron density profile (i.e. set of  $\alpha_j$ 's) should result in a set of  $r(\omega_i)$ 's which would match the set of data  $R(\omega_i)$ 's. Figure 18 illustrates the iterative procedure corresponding to successive solutions,  $[\alpha(z_j)]_{\text{new}}$ , to equation (80).

The set of  $r(\omega_i)$ 's, computed from each electron density profile (i.e. each successive set of  $[\alpha(z_j)]_{\text{new}}$ , are presented in figure 18 as the curves  $[r(\omega)]_1, [r(\omega)]_2$ , etc. The data values are shown in the figure as  $R(\omega_1), R(\omega_2)$ , etc.

In carrying through the iterative procedure to obtain a match between the computations and the data, it is noted the minimization requirement of equation (14) implies that the deviation between the  $r(\omega_i)$ 's and the  $R(\omega_i)$ 's be minimized. Following equation (15), this may be written as:

$$S = \sum_{i=1}^m \left( \frac{r(\omega_i) - R(\omega_i)}{\sigma_i} \right)^2 \rightarrow \text{minimum} \quad (82)$$

which demands that each frequency point on the  $r(\omega)$  curve pursue approximately the shortest course possible, in the complex plane, to get from the  $[r(\omega)]_1$  curve to the  $R(\omega_i)$ 's.

Observation of the curves, in figure 18, shows that the points of  $[r(\omega)]_1$  are numbered in the opposite sense to those of the data  $R(\omega_i)$ 's. The trend of the  $r(\omega)$  curves will need to include a complete reversal if a match to data is to be accomplished. The arrows which emanate from each  $r(\omega_i)$  point indicate the direction in which each  $r(\omega_i)$  point is constrained to move as the iterative steps progress toward the final match using the above definition of "s".

It is noted that in the sequence, shown in figure 18, that a loop is formed and then unwound. In forming a loop, however, the curve is forced to contain a "cusp" at one stage, as is shown on the curve  $[r(\omega)]_3$ . Experience with numerical computations has shown that in cases of this type the coefficient matrix of equation (80) becomes singular as the form of the curve containing the "cusp" is approached, and hence the solution for the  $\Delta\alpha_j$ 's, and thus for the electron density profile, diverges.

### G. Transformation Function, "g(r,ω)"

The sequence of  $r(\omega)$  curves in the above example need not include a curve containing a "cusp" if one end of the  $r(\omega)$  curve is rotated about the other. This does, however, require a different definition of the "s" of equation (82).

The definition of "s" required for this sequence must emphasize the angle assumed by the curve in the complex plane at each frequency point,  $r(\omega_i)$ , except at the end about which the curve is to be rotated. At this end point the absolute position of the point is to be stressed, as before. A complete definition of the curve must also include a requirement that the spacing of frequency points,  $r(\omega_i)$ , must match for the computed and data curves. It is then noted that since the low frequency end of the  $r(\omega)$  curve,  $r(\omega_1)$ , is more stable with respect to small changes in the electron density profile, it is likely to be the better choice for the end about which rotation is to be carried out.

A function,  $g(r)$ , containing the above properties is:

and

$$\left\{ \begin{array}{l} g_1 = r_1 \\ g_i = \ln \left( \frac{dr}{d\omega} \right)_i \quad ; \quad i = 2, \dots, m \end{array} \right\} \quad (83)$$

or

and

$$\left\{ \begin{array}{l} g_1 = r_1 (\text{real}) + j r_1 (\text{imag.}) \\ g_i = \ln \left| \left( \frac{dr}{d\omega} \right)_i \right| + j (\Phi_g)_i \end{array} \right\} \quad (84)$$

where  $i = 2, \dots, m$ ,  $j = \sqrt{-1}$

and

$$\phi_i = (\Phi_i \pm 2n_i \pi)$$

where  $\Phi_i$  is the principle part of the phase term and lies in the interval  $-\pi < \Phi \leq \pi$ .

Figure 19 illustrates the transformation function,  $g$ , in the  $r$ -plane.

The phase angle,  $\phi_g$ , may be written as:

$$(\phi_g)_i = \text{ARCTAN} \left( \frac{\text{Imag.} (dr/d\omega)_i}{\text{Real} (dr/d\omega)_i} \right) \quad (85)$$

The value of  $n_i$ , in the phase term, is chosen for each frequency so as to ensure that the phase,  $\phi_i$ , is continuous along the  $r(\omega)$  curve. This requirement leaves the value of  $n_i$  arbitrary for one frequency, e.g. the lowest frequency,  $\omega_1$ . The  $n_i$  value for this frequency, that is,  $n_1$ , is chosen so as to cause the curve to rotate in the desired sense (i.e. clockwise or counterclockwise).

The transformation function for the data values,  $R(\omega_i)$ , is introduced as:

and

$$\left\{ \begin{array}{l} G_1 = R_1(\text{real}) + j R_1(\text{imag.}) \\ G_i = \ln \left| \left( \frac{dR}{d\omega} \right)_i \right| + j (\phi_g)_i \end{array} \right\} \quad (86)$$

where  $i = 2, \dots, m$  and

$$(\phi_g)_i = (\Phi_G)_i \pm 2(n_g)_i \pi$$

The phase angle,  $\phi_G$ , may be written as:

$$(\phi_G)_i = \text{ARCTAN} \left( \frac{\text{Imag} \left( \frac{dR}{d\omega} \right)_i}{\text{Real} \left( \frac{dR}{d\omega} \right)_i} \right) \quad (87)$$

Note that at a "cusp", as in the curve  $[r(\omega)]_3$  of figure 18,  $(dr/d\omega) = 0$  and hence:

$$g = \ln \left( \frac{dr}{d\omega} \right) = -\infty + f \text{ (indeterminate)} \quad (88)$$

The new definition of "s", which emphasizes a small deviation between computed values,  $g_i$ , and data values,  $G_i$ , is given by equation (61) as:

$$s = \underbrace{g_i - G_i}_{\text{L} \rightarrow} \left[ \left( \frac{1}{\sigma_{ii}} \right) \right] \underbrace{\left( \frac{1}{\sigma_{ii}} \right)}_{\text{L} \rightarrow} \underbrace{\left( g_i - G_i \right)}_{\text{L} \rightarrow} \quad (61)$$

This formulation will not allow a "cusp" to form in the iteration scheme.

The solution for the  $\Delta\alpha_j$ 's, and hence the set of  $(\alpha_j)_{\text{new}}$ , is given by the formulation in section II-C using the function  $g(\omega)$ . The real and imaginary parts of the  $g(\omega)$  in the present section are to be identified as the real function  $g(\omega)$  of section II-C. The equation to be solved is equation (60). The choice of uncertainty matrix (i.e.  $(1/\sigma)$ ) for the data values,  $G(\omega_j)$ , is made as described in appendix D. The  $\underline{C}$  matrix and the  $V$ -vector of equation (60) are replaced with the new  $\underline{C}$  matrix and the new  $V$ -vector of equation (79). The derivative terms  $(\partial g_i / \partial \alpha_j)$  of equation (60) are discussed in another section of this report.

Figure 20 shows the sequence of curves,  $[r(\omega)]_k$ , that are the result of the reflection coefficient computations made using each  $(\alpha_j)$  new electron density profile obtained from the iterative scheme as applied to solutions of equation (60). It is observed in the figure that, although the sequence of computed point  $r(\omega_i)$  in the curve  $[r(\omega)]_1$  is completely reversed from that of the data points  $R(\omega_i)$ , the iterative procedure causes the successive curves (i.e.  $[r(\omega)]_2$ ,  $[r(\omega)]_3$  etc.) to undergo a transformation (i.e. counterclockwise rotation) that leads to the desired match between computation and data.

Note that this choice of function  $g(\omega)$  to replace  $r(\omega)$  is an intuitive one, and that, at best, probably only one sense of rotation (clockwise vs. counterclockwise) will avoid the singular coefficient matrix of equation (60). An example has been found, however, with the use of simulated data, when a correct choice of rotation sense led to convergence in the sequence of solutions to equation (60).

#### H. The Derivatives $(dr/d\omega)_i$ and $(dR/d\omega)_i$

There is a requirement for a method to define the derivatives  $(dr/d\omega)_i$  and  $(dR/d\omega)_i$  along the curves  $r(\omega)$  and  $R(\omega)$  when values are given only at the data frequencies  $\omega_i$ . These given values are  $r(\omega_i)$  and  $R(\omega_i)$  with  $i = 1, \dots, m$ . A way to satisfy this requirement is to use the interpolation scheme described in section II-B-2. The derivative,  $(dr/d\omega)_i$  [(or  $dR/d\omega)_i$ ], is defined in terms of a smooth curve drawn through the points  $r(\omega_i)$  [or  $R(\omega_i)$ ] by the interpolation scheme.

The smooth curve is represented in terms of closely spaced points  $r(\omega_k)$ , at an interval in frequency of  $\Delta\omega$ , which include the set of  $r(\omega_i)$ 's [or  $R(\omega_i)$ 's].

More precisely, the interpolation procedure assumes that values of  $\omega_k$  are chosen at  $k = 1, \dots, K$ . These  $\omega_k$  values are separated by the increment,  $\Delta\omega$ . It is also assumed that known values of the parameters  $r(\omega_i)$  [or  $R(\omega_i)$ ] exist at the  $\omega$  values,  $\omega_i$ , where  $i=1, \dots, n$ . Note that  $K$  will be greater than  $n$ . In the set of  $\omega_k$ 's there will exist values of  $\omega$  such that each  $\omega_i$  will correspond to an  $\omega_k$ .

In section II-B-2, it is shown that, using the interpolation scheme described, the variable  $\rho_k \equiv \rho(\omega_k)$  may be written as a linear combination of the values of the  $r(\omega_i)$ 's [or the  $R(\omega_i)$ 's]. This is expressed as in equation (32) as:

$$\downarrow \left( \rho_k \right) = \downarrow \left[ b_{k,i} \right] \cdot \downarrow \left( r_i ( \text{or } R_i ) \right) \quad (89)$$

At these values of  $\omega$  where an  $\omega_k$  is equal to an  $\omega_i$ , the value of  $\rho(\omega_k)$  will be equal to the  $r(\omega_i)$  [or  $R(\omega_i)$ ] value.

The derivative at one interpolation point,  $\omega_k$ , is defined in terms of the change in value of  $\rho(\omega)$  at the interpolation points preceding and following that point. That is:

$$\left( \frac{d \rho(\omega)}{d \omega} \right)_k = \left[ \frac{\rho(\omega_{k+1}) - \rho(\omega_{k-1})}{2 \cdot \Delta\omega} \right] \quad (90)$$

where  $\Delta\omega$  is the interpolation increment in frequency and the  $\rho(\omega_k)$ 's are the interpolated values.

It is also shown in section II-B-2, that the derivatives,  $(d\rho(\omega)/d\omega)_k$  are linear combinations of the values of  $r(\omega_i)$  [or  $R(\omega_i)$ ]. That is:

from equation (35):

$$\downarrow \left( \left( \frac{d\rho}{d\omega} \right)_k \right) = \downarrow \left[ \overset{\leftarrow}{\beta_{ki}} \right] \downarrow \left( \overset{\leftarrow}{r_i} \text{ (or } R_i) \right) \quad (91)$$

In particular, at the data frequencies,  $\omega_i$ ,

$$\downarrow \left( \left( \frac{d\rho}{d\omega} \right)_i \right) = \downarrow \left( \overset{\leftarrow}{\alpha_{ii'}} \right) \cdot \downarrow \left( \overset{\leftarrow}{r_{i'}} \right) \quad (92)$$

and similarly:

$$\downarrow \left( \left( \frac{dR}{d\omega} \right)_i \right) = \downarrow \left( \overset{\leftarrow}{\alpha_{ii'}} \right) \cdot \downarrow \left( \overset{\leftarrow}{R_{i'}} \right) \quad (93)$$

where

$$(\alpha_{ii'}) \equiv (\beta_{ki}) \quad (94)$$

for values of "k" where  $\omega_k$  corresponds to the data frequencies,  $\omega_i$ .

That is, since:

$$\downarrow \left[ \overset{\leftarrow}{\beta_{ki}} \right] = \begin{bmatrix} \beta_{11} & \dots & \beta_{1n} \\ \vdots & & \vdots \\ \beta_{k1} & \dots & \beta_{kn} \end{bmatrix} \quad (95)$$

and

$$\downarrow \stackrel{i' \rightarrow}{\left( a_{ii'} \right)} = \begin{pmatrix} a_{11} & \cdots & a_{1n} \\ \vdots & & \vdots \\ a_{n1} & \cdots & a_{nn} \end{pmatrix} \quad (96)$$

Then, only those rows of the  $\beta$  matrix, which correspond to those  $\omega$  values where  $\omega_k \equiv \omega_i$ , are substituted into equation (96) in the row positions to give values to the  $\alpha$  matrix.

For a given  $\omega_i$  value, equation (92) may be written:

$$\left( \frac{dr}{d\omega} \right)_i = \sum_{i'}^n (a_{ii'}) \cdot r_{i'} \quad (97)$$

Note also, that derivatives of  $(dr/d\omega)_i$  with respect to the electron density profile parameters,  $\alpha_j$ , are of the form:

$$\frac{\partial}{\partial \alpha_j} \left( \frac{dr}{d\omega} \right)_i = \sum_{i'}^n (a_{ii'}) \frac{\partial r_{i'}}{\partial \alpha_j} \quad (98)$$

The above procedure of determining values for  $(dr/d\omega)_i$  and  $(dR/d\omega)_i$  allows for the phase terms of equations (84) and (86) to be followed along the curves  $r(\omega)$  and  $R(\omega)$  so as to ensure continuity of phase in selecting the values of the  $n_i$  parameters in the functions  $g(\omega_i)$  and  $G(\omega_i)$ .

I. Following of the Phase Angle,  $\phi$ , Along the Curves,  $r(\omega)$  [or  $R(\omega)$ ], and Derivation of the Derivatives,  $(dg(\omega_i)/d\omega_i)$

The curve,  $r(\omega)$  [or  $R(\omega)$ ] of section III-F is defined in terms of the interpolation points of section III-H at frequencies,  $\omega_k$ , spaced  $\Delta\omega$  apart. From equation (84):

$$\ln \left( \frac{dr}{d\omega} \right)_k = \ln \left| \left( \frac{dr}{d\omega} \right)_k \right| + j \phi_k \quad (99)$$

and

$$\phi_k = (\Phi_k \pm 2n_k \pi) \quad (100)$$

where  $\Phi_k$  is the principal part and the  $n_k$ 's are chosen so that:

$$|\phi_k - \phi_{k-1}| \quad \text{and} \quad |\phi_k - \phi_{k+1}|$$

are taken as small along the  $g(\omega)$  [or  $G(\omega)$ ] curve to ensure continuous changes in phase.

At the data frequencies,  $\omega_i$ , equation (84) is:

$$g_i = \ln \left( \frac{dr}{d\omega} \right)_i \quad ; \quad i = 2, \dots, m \quad (101)$$

or

$$g_i = \ln \left| \left( \frac{dr}{d\omega} \right)_i \right| + j (\Phi_i \pm 2n_i \pi) \quad (102)$$

Now taking the derivative of equation (101) with respect to the electron density profile parameters,  $\alpha_j$ , gives:

$$\frac{\partial g_i}{\partial \alpha_j} = \frac{\partial}{\partial \alpha_j} \left[ \ln \left| \left( \frac{dr}{dw} \right)_i \right| \right] + \frac{\partial \Phi}{\partial \alpha_j} \quad (103)$$

Note that the number of cycles,  $n_i$ , are not relevant to the derivative.

At the data frequencies,  $(\omega_j)$ , equation (97) of section III-H may be substituted into equation (101) above to get for each  $g_i$ :

$$g_i = \ln \left\{ \sum_{i'}^m a_{ii'} \cdot r_{i'} \right\} \quad (104)$$

then, using the following identity:

$$\frac{d \ln(u)}{d \alpha} = \frac{1}{u} \frac{du}{d \alpha} \quad (105)$$

the derivative  $(dg_i/d\alpha_j)$  may be written:

$$\frac{\partial g_i}{\partial \alpha_j} = \frac{1}{\sum_{i'}^m (a_{ii'} \cdot r_{i'})} \sum_{i'}^m \left( a_{ii'} \frac{\partial r_{i'}}{\partial \alpha_j} \right) \quad (106)$$

where the  $(a_{ii'})$  values are given in equation (94) of section III-H and the  $(dr_{i'}/d\alpha_j)$  terms are given in equations (70-73) in section III-E.

#### IV. SUMMARY OF THE INVERSION TECHNIQUE WITH EXAMPLE USING SIMULATED DATA

As stated in the introduction, the approach taken in finding a best-fit electron density profile from data is an iterative technique which optimizes the trade-off between the deviation from data, represented by the value "s", and curvature in the wanted electron density profile, represented by the value of "c". The trade-off is given by the condition:

$$c + \lambda s \longrightarrow \text{minimum} \quad (107)$$

where " $\lambda$ " must be chosen for the optimum condition.

The actual equation to be solved in order to obtain the desired electron density profile is, from equation (60):

$$\begin{aligned} & \underbrace{\left\{ \hat{i} \left( C_{j,j} \right) + \lambda \hat{i} \left[ \frac{\partial g_i}{\partial \alpha_j} \right] \cdot \hat{i} \left( \frac{1}{\sigma_{ii}} \right) \cdot \hat{i} \left( \frac{1}{\sigma_{ii}} \right) \cdot \hat{i} \left[ \frac{\partial g_i}{\partial \alpha_j} \right] \right\} \cdot \hat{i} \left( \Delta \alpha_j \right)}_{K} \quad (108) \\ & = - \underbrace{\left\{ \hat{i} \left( C_{j,j} \right) \cdot \hat{i} \left( \alpha_j^0 \right) - \hat{i} \left( V_j \right) + \lambda \hat{i} \left[ \frac{\partial g_i}{\partial \alpha_j} \right] \cdot \hat{i} \left( \frac{1}{\sigma_{ii}} \right) \cdot \hat{i} \left( \frac{1}{\sigma_{ii}} \right) \cdot \hat{i} \left( g_i - G_i \right) \right\}}_{T} \end{aligned}$$

The terms  $(C_{j,j})$ ,  $(\partial g_i / \partial \alpha_j)$ ,  $(1/\sigma_{ii})$ ,  $(V)$ ,  $(g_i - G_i)$ ,  $(\alpha_j^0)$  and  $(\Delta \alpha_j)$  are all described in section III.

Equation (108) may be written:

$$\underbrace{K(\lambda, r(\omega)) \cdot (\Delta \alpha_j)}_{\sim} \rightarrow = T(\lambda, \alpha_j^0, r(\omega), R(\omega)) \quad (109)$$

where

$\underline{K}$  = The coefficient matrix, and is a function of the trade-off parameter, " $\lambda$ "; and also a function of the computed ionospheric reflection coefficient  $r(\omega)$ .

$\vec{T}$  = A vector which is a function of the above " $\lambda$ ", and  $r$ . It is also a function of the ionospheric reflection coefficient data,  $R(\omega)$ , and a function of the previous electron density profile,  $\alpha_j^0$ .

$\overrightarrow{(\Delta\alpha_j)}$  = A vector which represents the modifications to be added to the previous electron density profile for that step of the iteration scheme.

$\omega_i$  = The data frequency,  $i=1, \dots, m$ .

Equation (109) is solved for  $(\Delta\alpha_j)$  as:

$$\overrightarrow{(\Delta\alpha_j)} = \overrightarrow{(\underline{K})^{-1} \cdot \vec{T}} \quad (110)$$

Recall that  $(\alpha_j^0)$  refers to the previous electron density profile in the iteration scheme (e.g. the initial profile in the case of the first iteration step) and that  $(\Delta\alpha_j)$  is the solution to each iteration of equation (108) [or (110)]. The new profile generated by each iteration is:

$$\overrightarrow{(\alpha_j)} = \overrightarrow{(\alpha_j^0)} + \overrightarrow{(\Delta\alpha_j)} \quad (111)$$

where each term is a vector of length  $j=1, \dots, n$ , with  $n$  being the number of segments in the electron density profile.

A full wave computation, using each set of  $(\alpha_j)$ 's as the input profile, will give the set of reflection coefficients,  $r(\omega_i)$  needed in the inversion scheme.

An example of the inversion procedure is illustrated in figures 21, (a and b) and 22, (a and b). In particular, figure 21,a shows a data profile for which simulated reflection coefficient data was obtained by a full-wave computation. Also shown in the figure, is the starting profile used in the inversion technique. The positions of the profile "stops" are indicated in the figure.

Figure 21,b gives a comparison between the simulated  $R(\omega_i)$  data values, as obtained from the data profile, and the computed  $r(\omega_i)$  values from computations using the starting profile of figure 21,a. The data frequencies used were from 8 through 17 kHz at a frequency increment of 1 kHz. The 8 kHz computed value is identified by the box that encloses the number 1 while the 17 kHz value is identified by the box with the number 10. In this example it was assumed that the  $R(\omega_i)$  data was error free. The figure illustrates that the  $R(\omega_i)$  values and the  $r(\omega_i)$  values are very different at this initial step of the iteration.

Figure 22,a shows the comparison between the original data profile and the final profile obtained from the inversion scheme. Note in the figure that the top of the final profile has moved away from the original "stop" value, thus indicating that information exists in the data values that leads to this characteristic. The lowest value of the final profile remains at the stop value indicating that no information is available in the data to modify this relationship.

Figure 22,b illustrates the comparison between the data values ( $R(\omega_i)$ ) and the computed values ( $r(\omega_i)$ ) as obtained from the final profile of figure 22,a. In this case the  $r(\omega)$  curve has completely reversed in sequence from that shown in figure 21,b. This was accomplished by a counterclockwise rotation of the computed curve  $r(\omega)$  as the iterative sequence progressed.

Also, the spacing between the various  $r(\omega_i)$  values has been modified from that of figure 21,b so that the fit to the error-free simulated data,  $R(\omega_i)$ , appears to be very good.

It must be realized that the quality of fit, shown above, between the simulated data,  $R(\omega_i)$ , and the computed values,  $r(\omega_i)$ , as obtained from the inversion procedure, are done for the ideal case of no error in the  $R(\omega_i)$  values. Also, it was assumed that the electron-neutral particle collision frequency was known exactly. In cases where the input parameters are not as described in the above example, the results cannot be expected to be as outstanding. Examples of other cases, in which gaussian random error is added to the simulated data, are given in reference 8 which also describes the computer program which applies the inversion scheme described in this report. The quality of results obtained using actual experimental measurements is still to be determined.

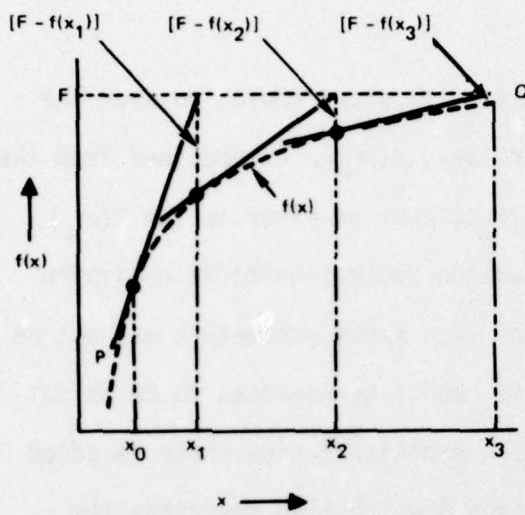


Figure 1. Newton-Raphson inversion of  $f(x) = F$  to get  $x$ .

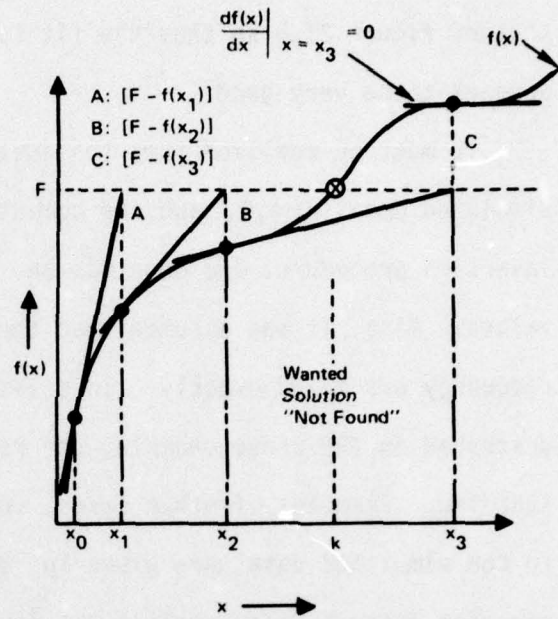


Figure 2. Newton-Raphson inversion of  $f(x) = F$  to get  $x$  where no solution is obtained.

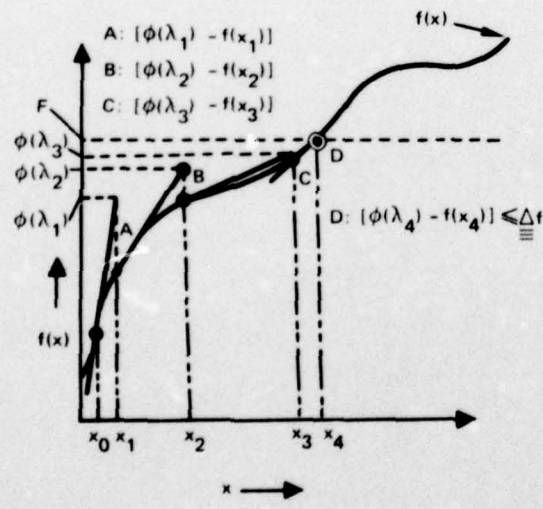


Figure 3. Modified Newton-Raphson inversion of  $f(x) = F$  to get  $x$ .

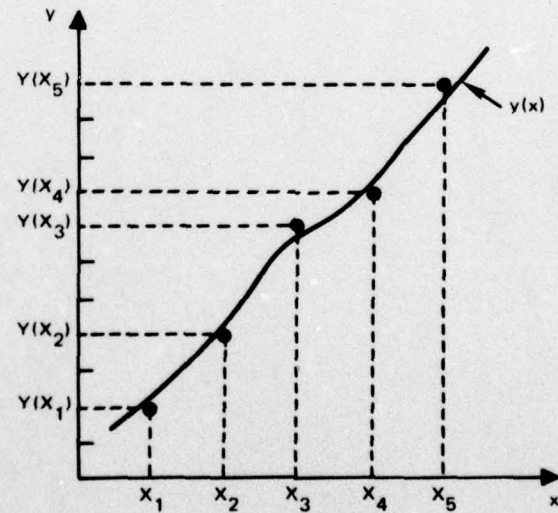


Figure 4. Plot of  $Y(X_i)$  data points illustrating the smoothing criteria.

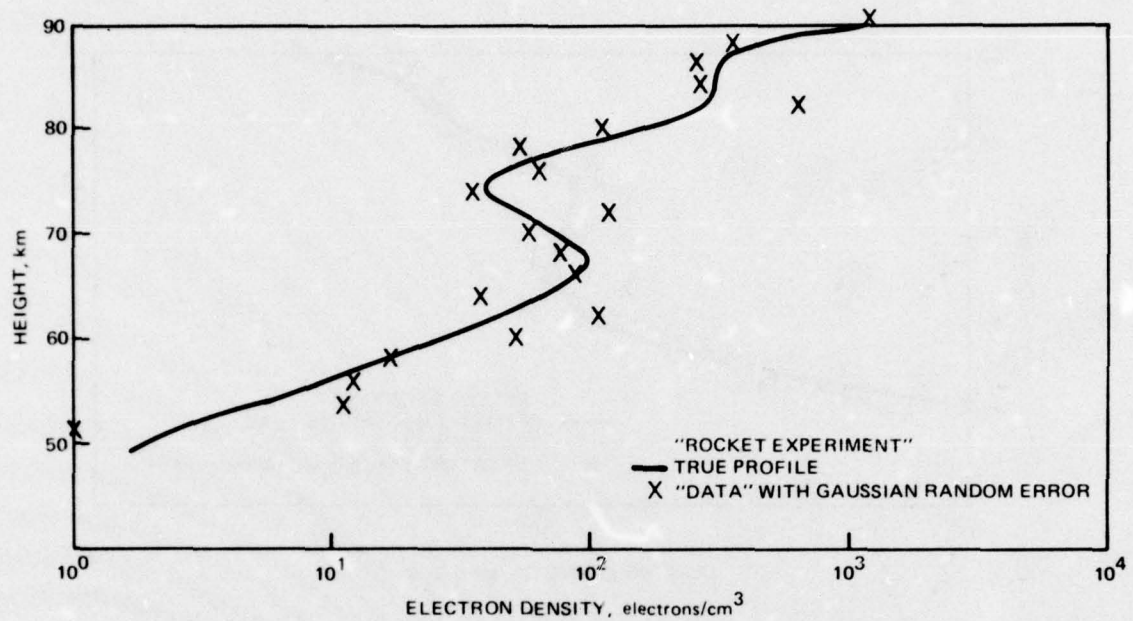


Figure 5. Comparison of true profile to data with added gaussian error.

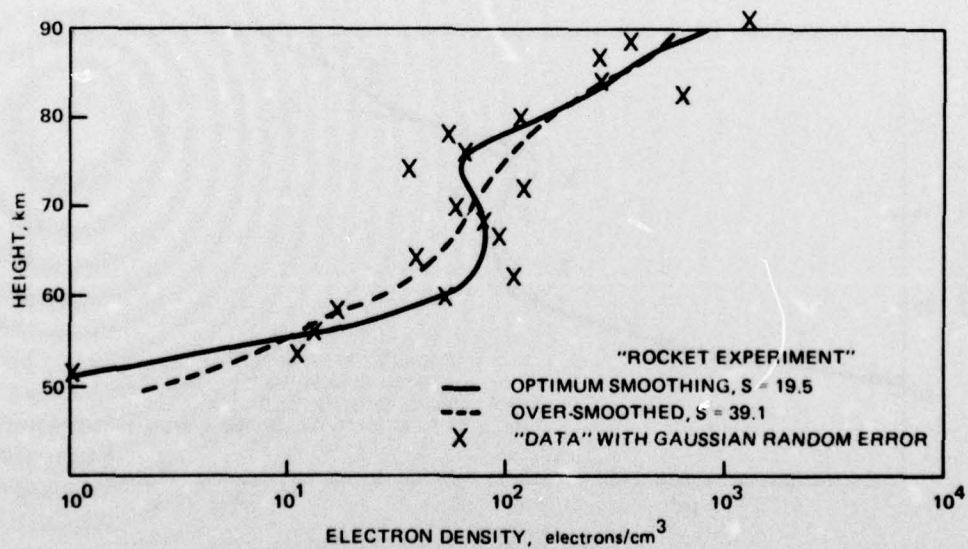


Figure 6. Comparison of optimally smoothed and over smoothed results to data with added gaussian error.

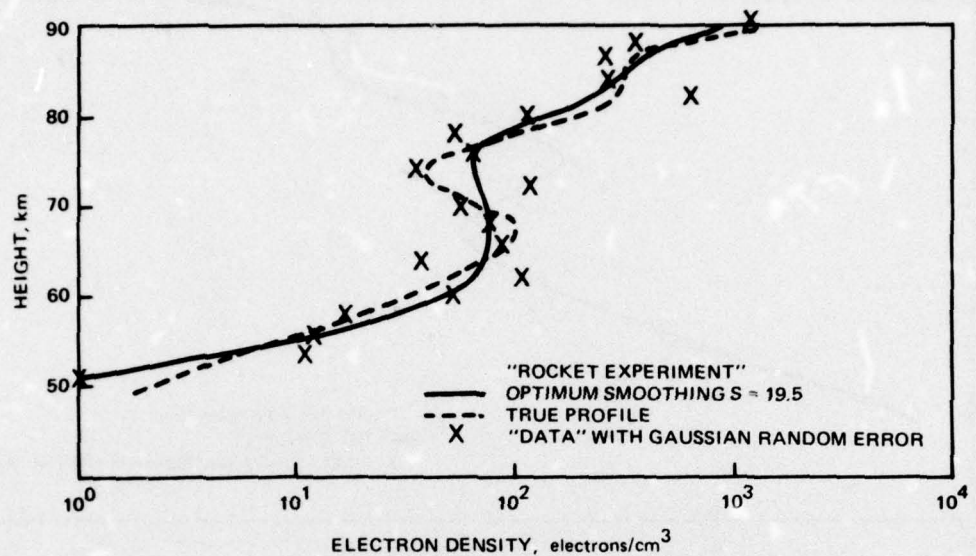


Figure 7. Comparison of optimally smoothed results to the true profile and to data with added gaussian error.

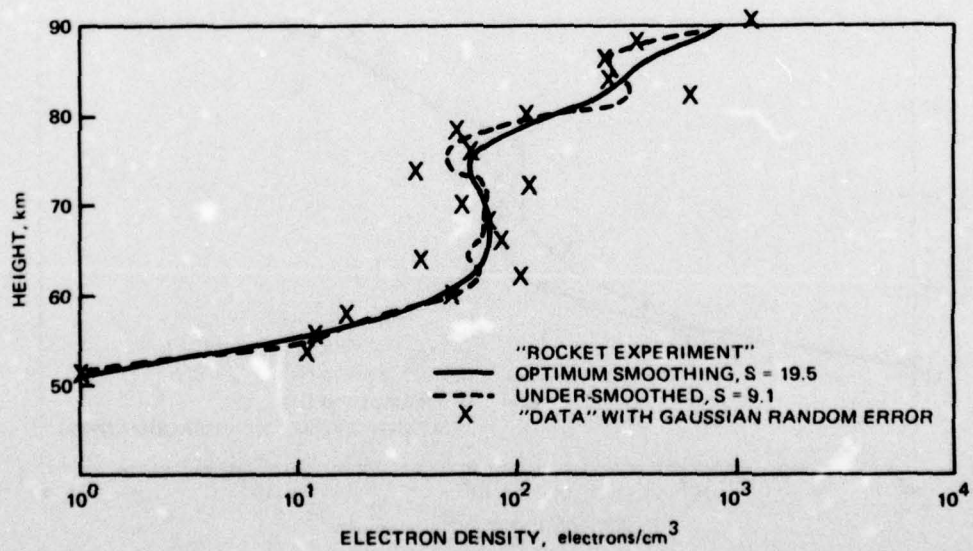


Figure 8. Comparison of optimally smoothed and undersmoothed results to data with added gaussian error.

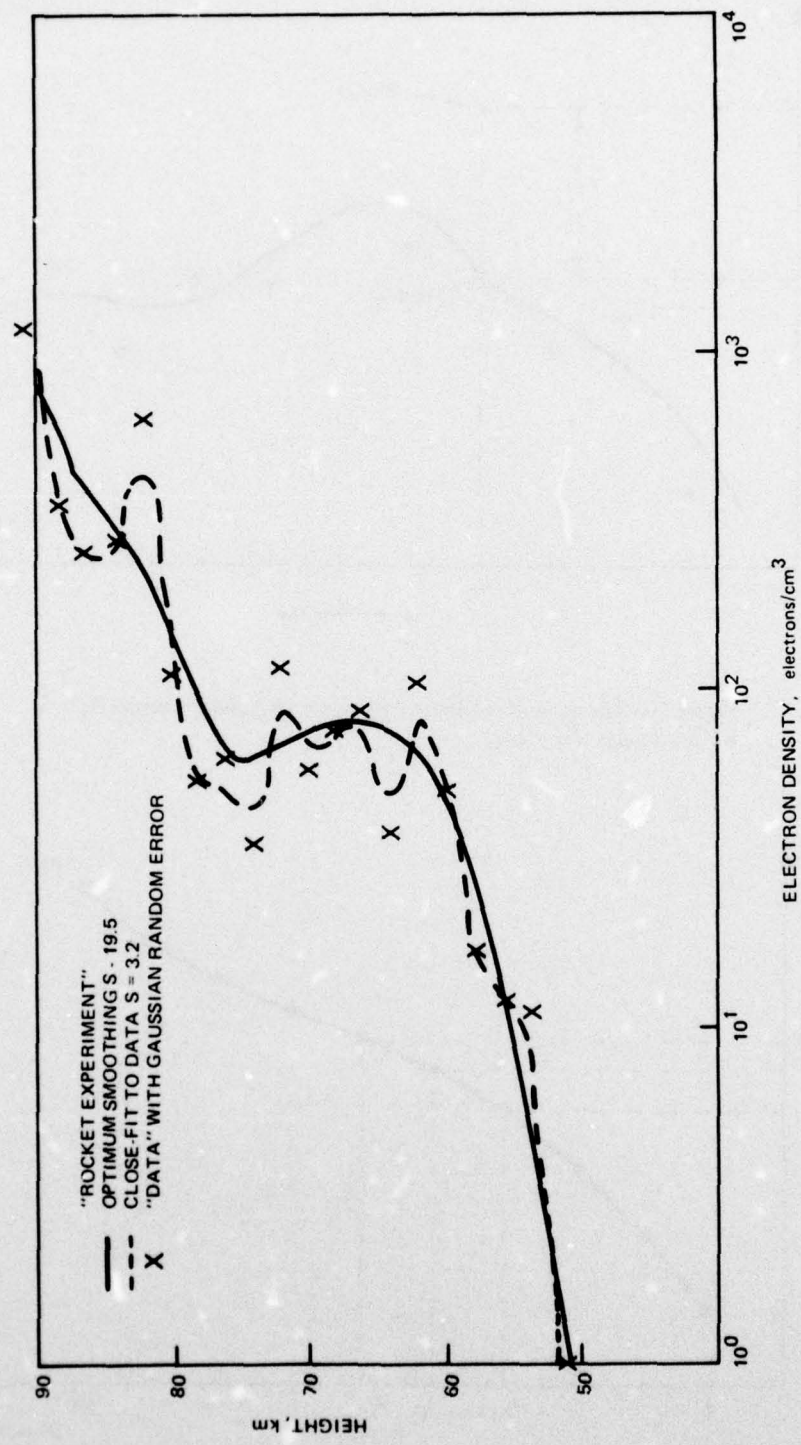


Figure 9. Comparison of optimally smoothed and greatly undersmoothed results to data with added gaussian error.

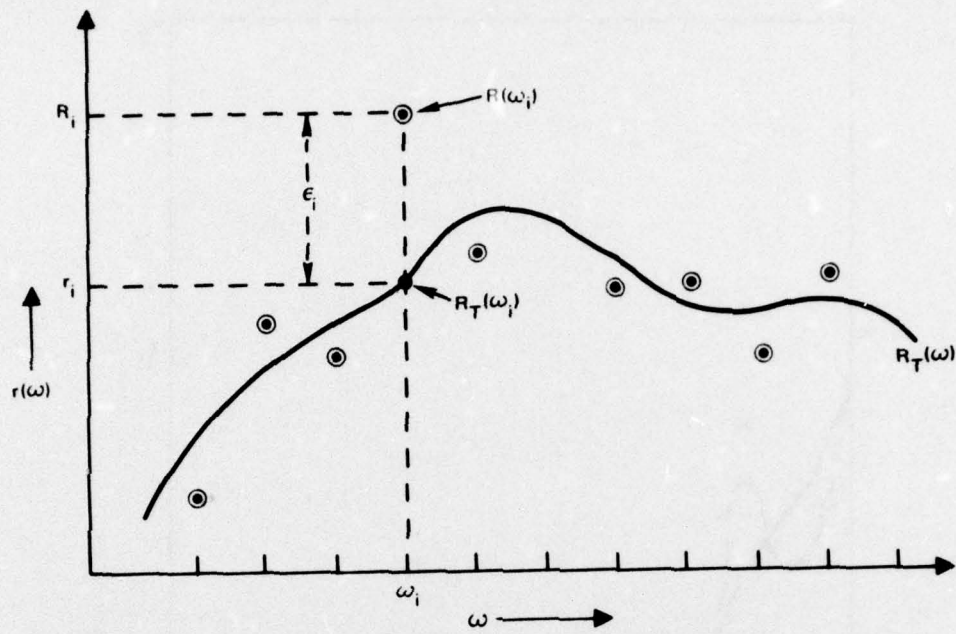


Figure 10. The curve  $R_T(\omega)$ , the data values ( $R_i$ ) and the errors ( $\epsilon_i$ ).  
 $R_T(\omega)$  implies true value.

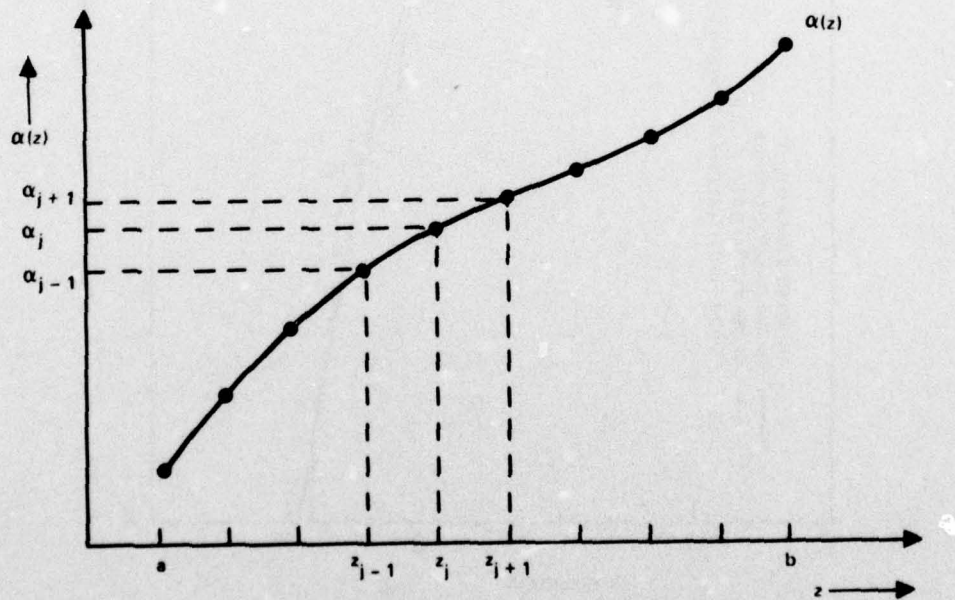


Figure 11. The curve,  $\alpha(z)$ , in terms of short segments,  $\alpha(z_j)$ .

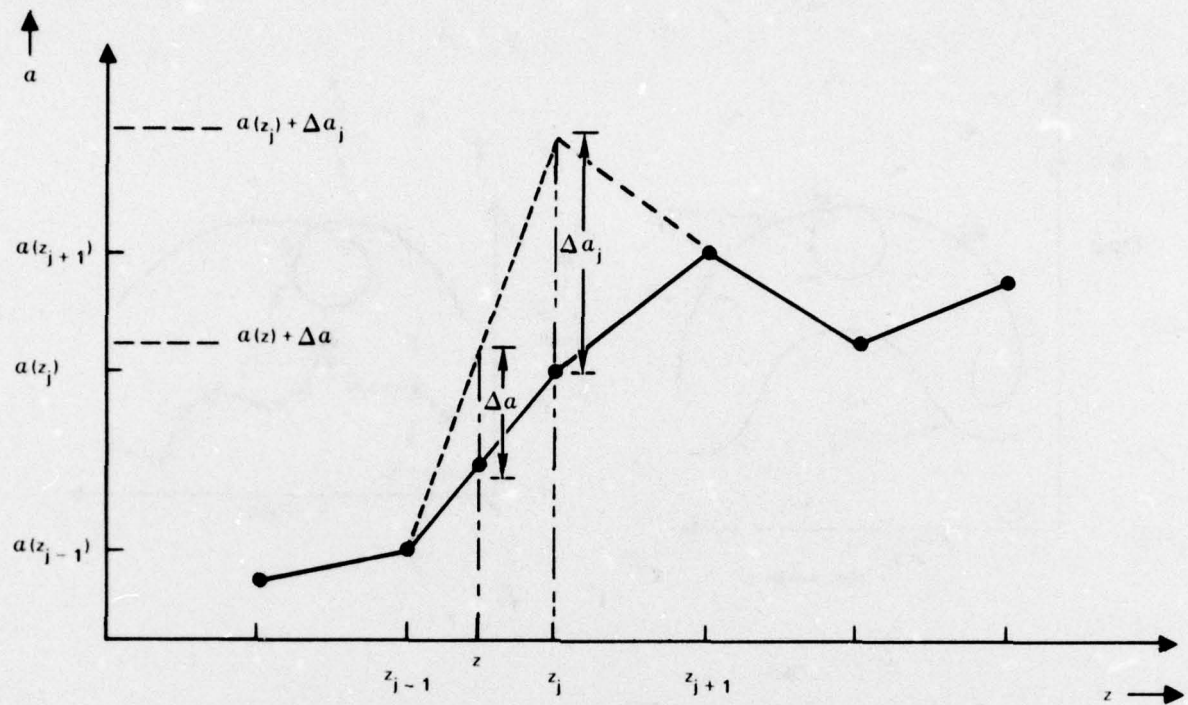


Figure 12. Increments associated with the weighting function ( $\partial a / \partial a_j$ ).

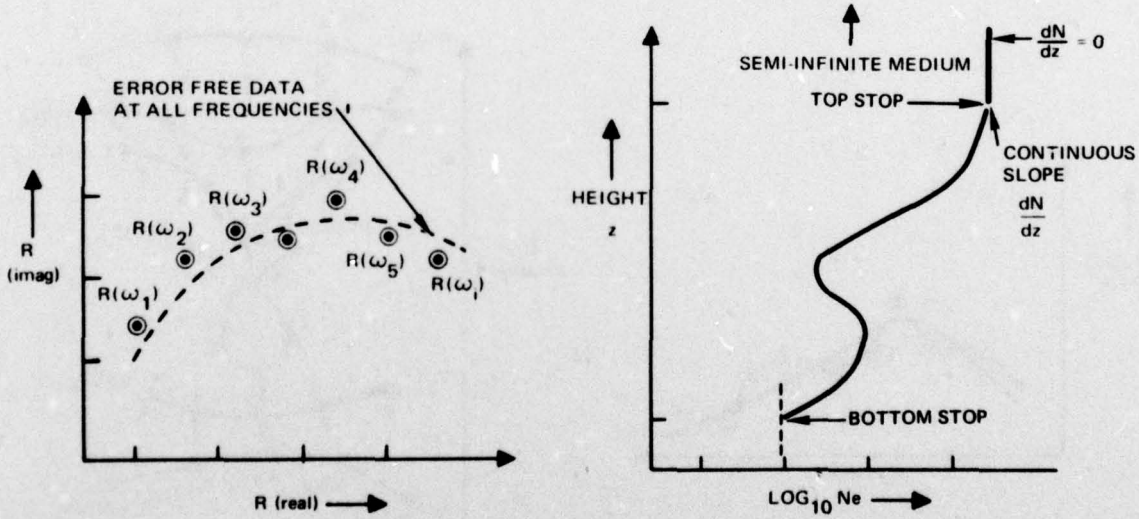


Figure 13. R-plane representation of  $R$  (real) and  $R$  (imaginary) data as a function of propagation frequency,  $\omega_j$ .

Figure 14. Constraints on the electron density profile.

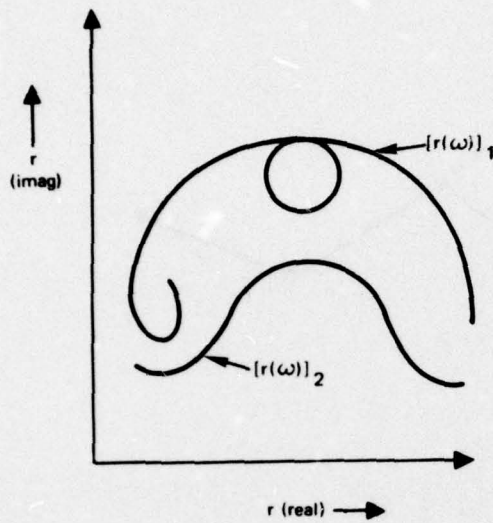


Figure 15.  $r$ -plane representation of  $r(\omega)$  (real) and  $r(\omega)$  (imaginary) as a function of propagation frequency.

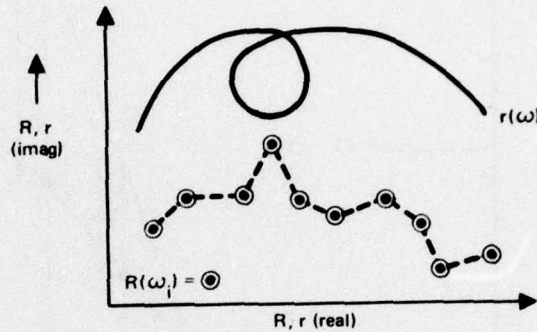


Figure 16. Comparison of  $R(\omega_i)$  reflection coefficient data and  $r(\omega)$  computations.

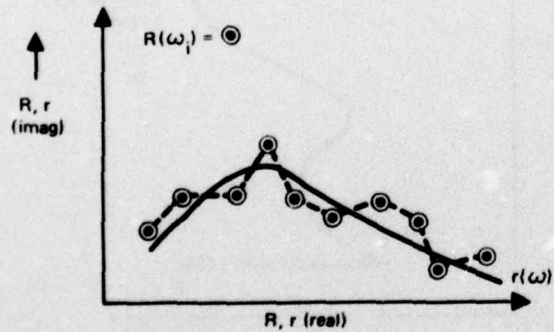


Figure 17. Matched comparison of  $R(\omega_i)$  reflection coefficient data and  $r(\omega)$  computations.

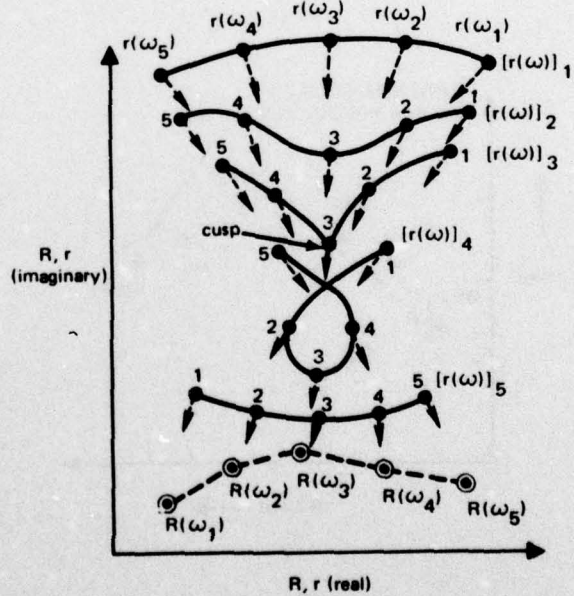


Figure 18. Possible sequence of  $r(\omega)$  iterations to obtain match between  $r(\omega_i)$  and  $R(\omega_i)$  values in which a "cusp" is allowed to form.

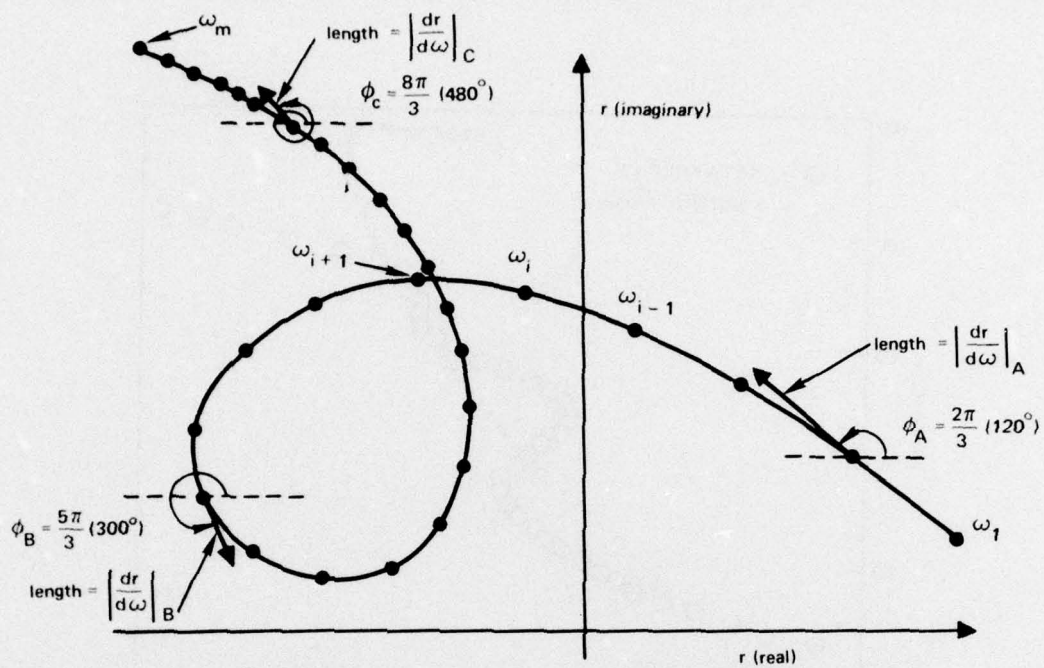


Figure 19. The  $r(\omega)$  curve illustrating the transformation function,  $g(\omega_i) = \ln \left| \frac{dr}{d\omega} \right|_i + j\phi_i$  (i.e., spacing and phase).

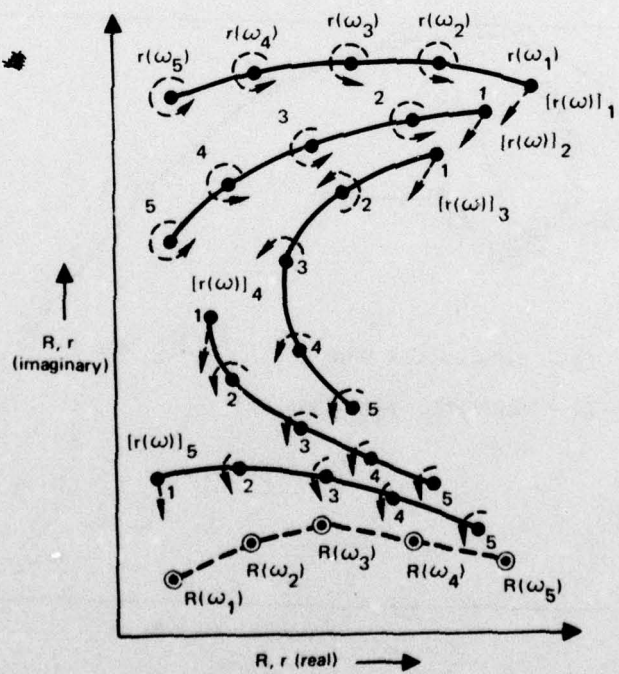


Figure 20. Sequence of  $r(\omega)$  iterations to obtain match between  $r(\omega_i)$  and  $R(\omega_i)$  values using the  $g$ -function.

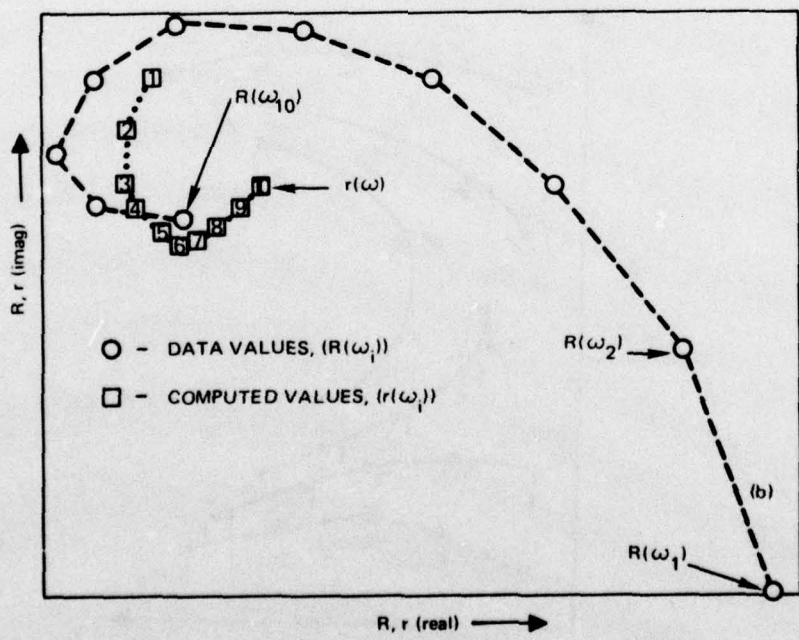
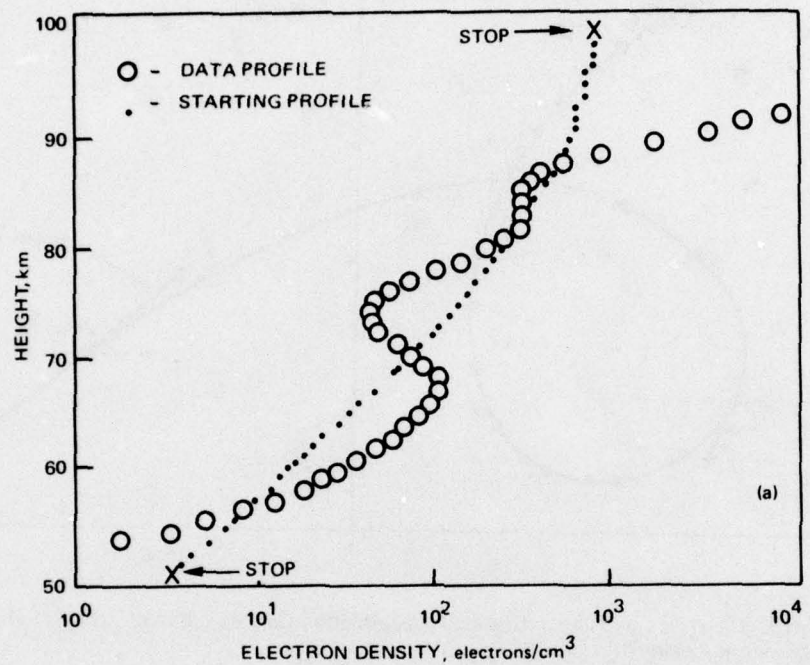


Figure 21. Comparison of simulated data and computed values for initial profile.

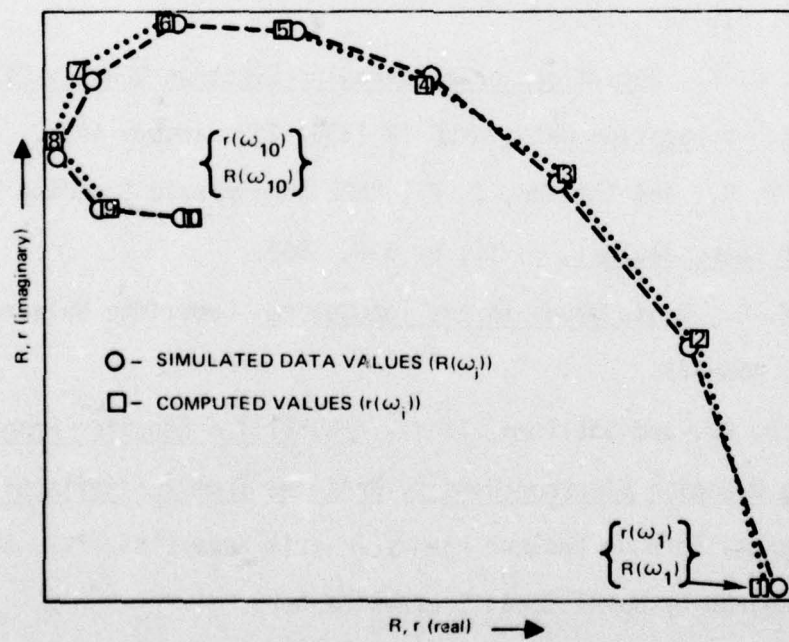
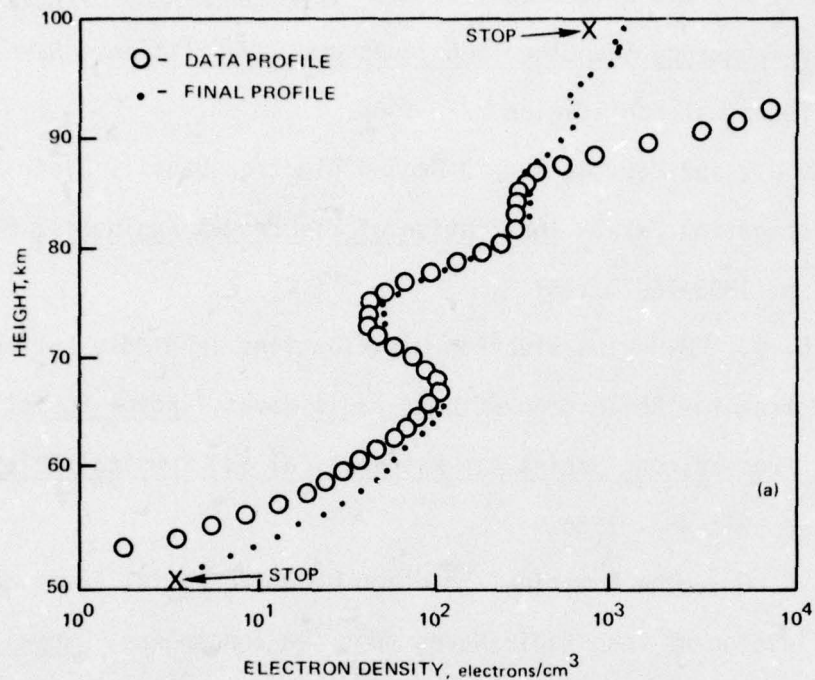


Figure 22. Inversion procedure, final iteration, for error-free simulated data.

## VI. References

1. Martin, J. N., and Hildebrand, V. E., Review of Steep-Incidence, VLF, Multiple-Frequency Sounding Techniques and Capabilities. Naval Weapons Center Technical Publication 772, 1968.
2. Bain, W. C., and May, B. R., "D-Region Electron-Density Distributions from Propagation Data," Institution of Electrical Engineers. Proceedings, V. 114, p. 1593-1597, 1967.
3. Deeks, D. G., "D-Region Electron Distributions in Middle Latitudes Deduced from the Reflection of Long Radio Waves," Royal Society of London. Proceedings. Series A: Mathematical and Physical Sciences V. 291, p. 413-437, 1966.
4. Budden, K. G., "The Numerical Solution of Differential Equations Governing Reflection of Long Radio Waves from the Ionosphere," Royal Society of London, Proceedings. Series A: Mathematical and Physical Sciences, V. 227, p. 516-537, 1955.
5. Shellman, C. H., Determination of D-Region Electron Density Distributions from Radio Propagation Data, NELC TR 1856, 23, January 1973.
6. Paulson, M. R., and Theisen, J. F., "NEL Ionospheric Sounding System," Bureau of Ships Journal, V. 11, p. 3-6, 1962.
7. Budden, K. G., Radio Waves in the Ionosphere, Cambridge University Press, 1961, pp. 460-463.
8. Morfitt, D. G., and Shellman, C. H., "INVERT," A Computer Program for Obtaining D-Region Electron Density Profiles from VLF Reflection Coefficients, Defense Nuclear Agency Interim Report No. 782, 30 November 1977, prepared by Naval Ocean Systems Center.

## VII. APPENDICES

### Appendix A. The "C" Matrix

In the procedure of smoothing out error in data of the form  $y(x)$  vs.  $x$ , a term identified as curvature is utilized.

The curvature term is defined as:

$$c = \int \left( \frac{d^2y}{dx^2} \right)^2 dx \quad (A-1)$$

Equation (A-1) refers to a continuous curve  $y(x)$ . However in practice,  $y(x)$  can only be specified at a finite number of points,  $x_j$  ( $j=1, \dots, n$ ). For simplicity it will be assumed that the  $x_j$ 's are equally spaced at intervals,  $\Delta x$ .

At the position  $x_j$  the curvature term is approximated by:

$$\frac{d^2y}{dx^2} \approx \left( \frac{y_{j-1} - y_j}{\Delta x} + \frac{y_j - y_{j+1}}{\Delta x} \right) / \Delta x \quad (A-2)$$

This term is illustrated in figure A-1.

The curvature function, "c", is then given by the expression:

$$c \approx \left\{ \sum_{j=2}^{n-1} (y_{j-1} - 2y_j + y_{j+1})^2 \right\} / (\Delta x)^3 \quad (A-3)$$

where  $n$  is the number of points,  $x_j$ .

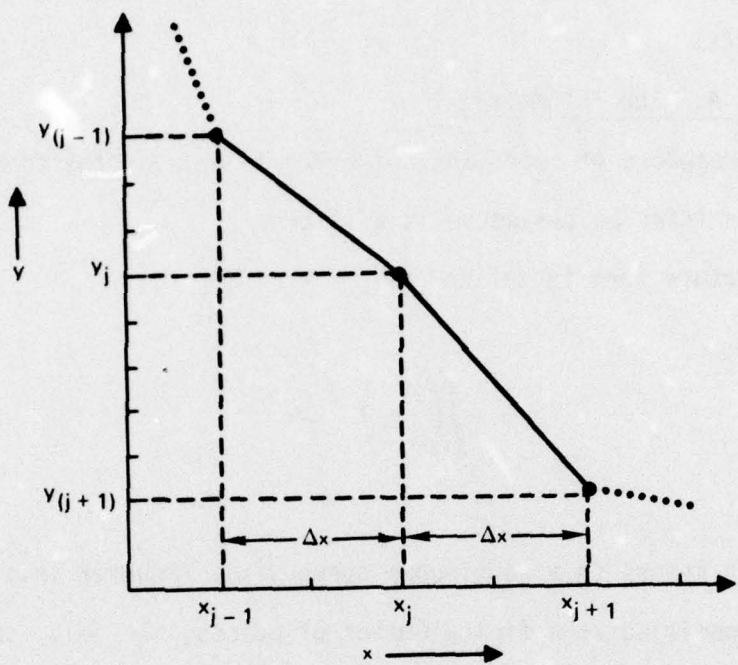


Figure A-1. Plot of  $y(x)$  for curvature.

Note that the expression:

$$(y_{j-1} - 2y_j + y_{j+1})^2$$

can be written as:

$$[(y_{j-1})^2 + 4(y_j)^2 + (y_{j+1})^2 - 4(y_{j-1} y_j) - 4(y_j y_{j+1}) + 2(y_{j-1} y_{j+1})]$$

(A-4)

For illustration, let  $n = 8$  and expand the expression (A-4). This gives,  
from equation (A-3):  $(\Delta X)^2 \cdot C =$

$$\begin{aligned}
 & (y_1)^2 + 4(y_2)^2 + (y_3)^2 - 4(y_1 y_2) - 4(y_2 y_3) + 2(y_1 y_3) \\
 & + (y_2)^2 + 4(y_3)^2 + (y_4)^2 - 4(y_2 y_3) - 4(y_3 y_4) + 2(y_2 y_4) \\
 & + (y_3)^2 + 4(y_4)^2 + (y_5)^2 - 4(y_3 y_4) - 4(y_4 y_5) + 2(y_3 y_5) \\
 & + (y_4)^2 + 4(y_5)^2 + (y_6)^2 - 4(y_4 y_5) - 4(y_5 y_6) + 2(y_4 y_6) \\
 & + (y_5)^2 + 4(y_6)^2 + (y_7)^2 - 4(y_5 y_6) - 4(y_6 y_7) + 2(y_5 y_7) \\
 & + (y_6)^2 + 4(y_7)^2 + (y_8)^2 - 4(y_6 y_7) - 4(y_7 y_8) + 2(y_6 y_8)
 \end{aligned}$$

Rearranging terms gives

(A-5)

$$(\Delta X)^2 \cdot C =$$

$$\begin{aligned}
 & y_1 y_2 - 2 y_1 y_3 + y_1 y_5 \\
 & - 2 y_2 y_3 + 5 y_2 y_4 - 4 y_2 y_5 + y_2 y_7 \\
 & + y_3 y_1 - 4 y_3 y_2 + 6 y_3 y_3 - 4 y_3 y_4 + y_3 y_6 \\
 & + y_4 y_2 - 4 y_4 y_3 + 6 y_4 y_4 - 4 y_4 y_5 + y_4 y_8 \\
 & + y_5 y_3 - 4 y_5 y_4 + 6 y_5 y_5 - 4 y_5 y_6 + y_5 y_7 \\
 & + y_6 y_4 - 4 y_6 y_5 + 6 y_6 y_6 - 4 y_6 y_7 + y_6 y_8 \\
 & + y_7 y_5 - 4 y_7 y_6 + 5 y_7 y_7 - 2 y_7 y_8 \\
 & + y_8 y_6 - 2 y_8 y_7 + y_8 y_8
 \end{aligned}$$

(A-6)

In matrix notation equation (A-6) may be written as:

(A-7)

$$(\Delta X)^3 \cdot C =$$

$y_1 \ y_2 \ y_3 \ y_4 \ y_5 \ y_6 \ y_7 \ y_8$

$$\begin{pmatrix} 1 & -2 & 1 & 0 & 0 & 0 & 0 & 0 \\ -2 & 5 & -4 & 1 & 0 & 0 & 0 & 0 \\ 1 & -4 & 6 & -4 & 1 & 0 & 0 & 0 \\ 0 & 1 & -4 & 6 & -4 & 1 & 0 & 0 \\ 0 & 0 & 1 & -4 & 6 & -4 & 1 & 0 \\ 0 & 0 & 0 & 1 & -4 & 6 & -4 & 1 \\ 0 & 0 & 0 & 0 & 1 & -4 & 5 & -2 \\ 0 & 0 & 0 & 0 & 0 & 1 & -2 & 1 \end{pmatrix} \cdot \begin{pmatrix} y_1 \\ y_2 \\ y_3 \\ y_4 \\ y_5 \\ y_6 \\ y_7 \\ y_8 \end{pmatrix}$$

or

$$(\Delta X)^3 \cdot C = \underbrace{y_{j'}}_{\substack{i' \rightarrow \\ \downarrow}} \cdot \underbrace{i' \left( \begin{matrix} C \\ \downarrow \end{matrix} \right)}_{\substack{i \rightarrow \\ \downarrow}} \cdot \underbrace{i \left( y_i \right)}_{\substack{i \rightarrow \\ \downarrow}} \quad (A-8)$$

where  $j' = 1, \dots, n$  and  $j = 1, \dots, n$

or  $j' = 1, \dots, 8$  or  $j = 1, \dots, 8$

Also

$$\underbrace{y_{j'}}_{\substack{i' \rightarrow \\ \downarrow}} \quad \text{is a } 1 \times 8 \text{ row vector}$$

$$\underbrace{i' \left( \begin{matrix} C \\ \downarrow \end{matrix} \right)}_{\substack{i \rightarrow \\ \downarrow}} \quad \text{is an } 8 \times 8 \text{ matrix}$$

$$\underbrace{i \left( y_i \right)}_{\substack{i \rightarrow \\ \downarrow}} \quad \text{is a } 8 \times 1 \text{ column vector}$$

### Appendix B. The Derivatives of the Curvature Term "c"

From appendix A, the expression of the curvature term "c" is given by equation (A-5). In the illustrative case given there,  $n = 8$ . The first derivative terms are:

$$\left. \begin{array}{l} \frac{\partial c}{\partial y_1} = 2y_1 - 4y_2 + 2y_3 \\ \frac{\partial c}{\partial y_2} = -4y_1 + 10y_2 - 8y_3 + 2y_4 \\ \frac{\partial c}{\partial y_3} = 2y_1 - 8y_2 + 12y_3 - 8y_4 + 2y_5 \\ \frac{\partial c}{\partial y_4} = 2y_2 - 8y_3 + 12y_4 - 8y_5 + 2y_6 \\ \frac{\partial c}{\partial y_5} = 2y_3 - 8y_4 + 12y_5 - 8y_6 + 2y_7 \\ \frac{\partial c}{\partial y_6} = 2y_4 - 8y_5 + 12y_6 - 8y_7 + 2y_8 \\ \frac{\partial c}{\partial y_7} = 2y_5 - 8y_6 + 10y_7 - 4y_8 \\ \frac{\partial c}{\partial y_8} = 2y_6 - 4y_7 + 2y_8 \end{array} \right\} \quad (B-1)$$

In matrix notation the derivative terms can be written as:

$$\left. \begin{array}{l} \frac{\partial c}{\partial y_1} \frac{\partial c}{\partial y_2} \frac{\partial c}{\partial y_3} \frac{\partial c}{\partial y_4} \frac{\partial c}{\partial y_5} \frac{\partial c}{\partial y_6} \frac{\partial c}{\partial y_7} \frac{\partial c}{\partial y_8} = \\ y_1 \ y_2 \ y_3 \ y_4 \ y_5 \ y_6 \ y_7 \ y_8 \end{array} \right\} \quad (B-2)$$

$$\begin{pmatrix} 2 & -4 & 2 & 0 & 0 & 0 & 0 & 0 \\ -4 & 10 & -8 & 2 & 0 & 0 & 0 & 0 \\ 2 & -8 & 12 & -8 & 2 & 0 & 0 & 0 \\ 0 & 2 & -8 & 12 & -8 & 2 & 0 & 0 \\ 0 & 0 & 2 & -8 & 12 & -8 & 2 & 0 \\ 0 & 0 & 0 & 2 & -8 & 12 & -8 & 2 \\ 0 & 0 & 0 & 0 & 2 & -8 & 10 & -4 \\ 0 & 0 & 0 & 0 & 0 & 2 & -4 & 2 \end{pmatrix}$$

Therefore the derivative terms of "c" may be written as:

$$(\Delta X)^3 \underbrace{\frac{\partial c}{\partial y_j}}_{j \rightarrow} = 2 \cdot \underbrace{y_{j'}}_{j' \rightarrow} \downarrow \left( C_{j'j} \right) \quad (B-3)$$

where  $j' = 1, \dots, 8$

and  $j = 1, \dots, 8$

It is of interest to note that the second derivative of "c" with respect to  $y_j$  is:

$$\frac{\Delta X^3}{2} \downarrow \left( \frac{\partial^2 c}{\partial y_{j'} \partial y_j} \right) = \downarrow \left( C_{j'j} \right) \quad (B-4)$$

### Appendix C. The Derivative Terms $(dy/dx)_j$

Given a set of data values  $Y(X_i)$ , ( $i = 1, \dots, m$ ), at each point  $X_i$ . It is required to find a set of interpolated values  $y(x_j)$ , ( $j = 1, \dots, n$ ), where the  $x_j$  are evenly spaced increments,  $\Delta x$ , of  $x$ . It is required that the set of  $y(x_j)$  values include the set of  $Y(X_i)$ 's. That is each  $Y(X_i)$  must also be a  $y(x_j)$ .

From equation (29) of section II-B-2, the relationship between the  $Y(X_i)$ 's and  $y(x_j)$ 's is:

$$\vec{y}' \left( \overset{j}{\vec{C}_{j'j}} \right) \overset{\text{mod}}{\vec{y}} = \vec{y}' \left( \vec{V}_{j'} \right) \quad (C-1)$$

where

$$y_j = Y(X_j)$$

where the  $j'$ -th row of  $(C_{j'j})^{\text{mod}}$  is the  $j'$ -th row of the matrix  $C$  of equation (22), if  $y(x_j)$  does not correspond to an  $Y(X_i)$ . If  $y(x_j)$  does correspond to an  $Y(X_i)$ , then the  $j'$ -th row of  $(C_{j'j})^{\text{mod}}$  is all zeros except for a 1 for the main diagonal element,  $C_{j'j'}$ . Also all the elements of the vector  $V_{j'}$  are zero except that if  $y(x_j)$  corresponds to an  $Y(X_i)$ , then  $V_{j'} = Y(X_i)$ . Equation (30) of section II-B-2 is an example of these relationships.

Now rewrite equation (C-1) as

$$\begin{array}{c} \overset{i \rightarrow}{\downarrow} \left( \begin{array}{c} C_{j \neq i} \\ \text{mod.} \end{array} \right) \quad \overset{i \rightarrow}{\downarrow} \left[ b_{jL} \right] \quad \overset{i \rightarrow}{\downarrow} \left( Y_i \right) \quad \overset{i \rightarrow}{\downarrow} \left[ v_{j \neq i} \right] \quad \overset{i \rightarrow}{\downarrow} \left( Y_i \right) \end{array} \quad (C-2)$$

where

$$Y_i = Y(X_i)$$

and where

$$\overset{i \rightarrow}{\downarrow} \left[ b_{jL} \right] \cdot \overset{i \rightarrow}{\downarrow} \left( Y_i \right) = \overset{i \rightarrow}{\downarrow} \left( y_j \right) \quad (C-3)$$

and also

$$\overset{i \rightarrow}{\downarrow} \left[ v_{j \neq i} \right] \cdot \overset{i \rightarrow}{\downarrow} \left( Y_i \right) = \overset{i \rightarrow}{\downarrow} \left( V_j \right) \quad (C-4)$$

so  $(y_j)$  is chosen to be such that it contains no  $Y_i$ 's.

$$(v_{jL}) = \begin{cases} 1 & \text{if } y_j = Y_i \\ 0 & \text{if } y_j \neq Y_i \end{cases} \quad (C-5)$$

Now consider equation (C-2) with the vector,  $(Y_i)$  omitted from both sides of the equation. This is:

$$\downarrow \begin{bmatrix} \vec{i} \\ \vec{C'_{jL}} \\ \vec{m_{cd}} \end{bmatrix} \cdot \downarrow \begin{bmatrix} \vec{i} \\ \vec{b_{jL}} \end{bmatrix} = \downarrow \begin{bmatrix} \vec{i} \\ \vec{v_{jL}} \end{bmatrix} \quad (C-6)$$

which contains no  $Y_i$ 's, but which may be solved for  $b_{jL}$ , that is:

$$\downarrow \begin{bmatrix} \vec{i} \\ \vec{b_{jL}} \end{bmatrix} = \downarrow \begin{bmatrix} \vec{i} \\ \left( \vec{C'_{jL}} \right)^{-1} \\ \vec{m_{cd}} \end{bmatrix} \cdot \downarrow \begin{bmatrix} \vec{i} \\ \vec{v_{jL}} \end{bmatrix} \quad (C-7)$$

Once the  $(b_{jL})$ 's are known, the  $y_j$ 's may be found from equation (C-3).

$$\downarrow \begin{bmatrix} \vec{y_j} \end{bmatrix} = \downarrow \begin{bmatrix} \vec{i} \\ \vec{b_{jL}} \end{bmatrix} \cdot \downarrow \begin{bmatrix} \vec{Y_L} \end{bmatrix} \quad (C-8)$$

This equation illustrates that the interpolated values,  $y_j$ , may be found from a linear combination of the data values,  $Y_i$ . That is:

$$y_j = \sum_i^m (b_{jL}) Y_i \quad (C-9)$$

Now consider a way of defining  $(dy/dx)_j$  in terms of  $y_j$  values. Let

$$\left(\frac{dy}{dx}\right)_j = \frac{(y_{j+1} - y_{j-1})}{2\Delta x} \quad (C-10)$$

Since from equation (C-9)

$$y_j = \sum_i^m (b_{j,i}) \cdot Y_i \quad (C-9)$$

where  $j = 1, \dots, n$ , a derivative at any interior point  $y_j$  may be defined as:

$$\left(\frac{dy}{dx}\right)_j = \frac{(y_{j+1} - y_{j-1})}{2\Delta x} = \frac{\sum_i^m (b_{j+1,i}) Y_i - \sum_i^m (b_{j-1,i}) Y_i}{2\Delta x} \quad (C-11)$$

or

$$\left(\frac{dy}{dx}\right)_j = \sum_i^m \frac{(b_{j+1,i} - b_{j-1,i}) Y_i}{2\Delta x} \quad (C-12)$$

$j = 2, \dots, n-1$

This equation may be written as:

$$\left(\frac{dy}{dx}\right)_j = \sum_i^m (\beta_{j,i}) Y_i \quad (C-13)$$

where

$$\beta_{j,i} = \frac{(b_{j+1,i} - b_{j-1,i})}{2\Delta x} \quad (C-14)$$

Appendix D. The Uncertainty Matrix,  $[1/\sigma]$

Given equation (54) of the main text as:

$$\begin{aligned} & \left\{ \underset{\text{mod.}}{\underset{\downarrow}{\mathbf{C}'_{ijj}}} + \lambda \underset{\downarrow}{\mathbf{z}} \left[ \frac{\partial r_i}{\partial \alpha_j} \right] \cdot \underset{\downarrow}{\mathbf{i}} \left( \frac{-1}{\sigma_{ii}^2} \right) \cdot \underset{\downarrow}{\mathbf{i}} \left( \frac{-1}{\sigma_{ii}^2} \right) \cdot \underset{\downarrow}{\mathbf{i}} \left[ \frac{\partial r_i}{\partial \alpha_j} \right] \cdot \underset{\downarrow}{\mathbf{z}} \left( \Delta \alpha_j \right) \right\} \\ & = - \left\{ \underset{\text{mod.}}{\underset{\downarrow}{\mathbf{C}'_{ijj}}} \cdot \underset{\downarrow}{\mathbf{z}} \left( \alpha_j^0 \right) - \underset{\downarrow}{\mathbf{i}} \left( V_j \right) + \lambda \underset{\downarrow}{\mathbf{z}} \left[ \frac{\partial r_i}{\partial \alpha_j} \right] \underset{\downarrow}{\mathbf{i}} \left( \frac{-1}{\sigma_{ii}^2} \right) \underset{\downarrow}{\mathbf{i}} \left( \frac{-1}{\sigma_{ii}^2} \right) \underset{\downarrow}{\mathbf{i}} \left( r_i^0 - R_i \right) \right\} \end{aligned} \quad (D-1)$$

where  $\left( \frac{-1}{\sigma_{ii}^2} \right)$  is a diagonal matrix with real constant elements. Also  $R_i$  is a data value,  $r_i$  is a computed value of the curve  $r(\omega)$  and  $\Delta \alpha_j \equiv \alpha(z_j) - \alpha^0(z_j)$ .

Consider the left side of equation (D-1). This may be written as:

$$\begin{aligned} & \left\{ \underset{\text{mod.}}{\underset{\downarrow}{\mathbf{C}'}} + \lambda \underset{\downarrow}{\mathbf{z}} \left[ \frac{\partial r_i}{\partial \alpha_j} \right] \cdot \underset{\text{unit matrix}}{\underset{\leftarrow \rightarrow}{\left[ \underset{\downarrow}{\mathbf{i}} \left( \frac{\partial g_{i''}}{\partial r_i} \right) \cdot \underset{\downarrow}{\mathbf{i}} \left[ \left( \frac{\partial g_{i''}}{\partial r_i} \right)^{-1} \right] \right]}} \cdot \underset{\downarrow}{\mathbf{i}} \left( \frac{-1}{\sigma_{ii}^2} \right) \right\} \\ & \underset{\text{unit matrix}}{\underset{\leftarrow \rightarrow}{\left[ \underset{\downarrow}{\mathbf{i}} \left( \frac{\partial g_{i''}}{\partial r_i} \right)^{-1} \right]}} \cdot \underset{\downarrow}{\mathbf{i}} \left( \frac{\partial g_{i''}}{\partial r_i} \right) \underset{\downarrow}{\mathbf{i}} \left[ \frac{\partial r_i}{\partial \alpha_j} \right] \cdot \underset{\downarrow}{\mathbf{z}} \left( \Delta \alpha_j \right) \end{aligned} \quad (D-2)$$

Note in equation (D-2) that:

$$\downarrow \left[ \begin{array}{c} \overset{i}{\rightarrow} \\ \dot{i} \left[ \frac{\partial r_i}{\partial \alpha_i} \right] \end{array} \right] \cdot \downarrow \left[ \begin{array}{c} \overset{i''}{\rightarrow} \\ \dot{i} \left( \frac{\partial g_{i''}}{\partial r_i} \right) \end{array} \right] = \downarrow \left[ \begin{array}{c} \overset{i''}{\rightarrow} \\ \dot{i} \left[ \frac{\partial g_{i''}}{\partial \alpha_i} \right] \end{array} \right] \quad (D-3)$$

And:

$$\downarrow \left[ \begin{array}{c} \overset{i''}{\rightarrow} \\ \dot{i} \left( \frac{\partial g_{i''}}{\partial r_i} \right) \end{array} \right] \downarrow \left[ \begin{array}{c} \overset{i}{\rightarrow} \\ \dot{i} \left[ \frac{\partial r_i}{\partial \alpha_i} \right] \end{array} \right] = \downarrow \left[ \begin{array}{c} \overset{i}{\rightarrow} \\ \dot{i} \left[ \frac{\partial g_{i''}}{\partial \alpha_i} \right] \end{array} \right] \quad (D-4)$$

Also, consider the following products of equation (D-2):

$$\downarrow \left[ \begin{array}{c} \overset{i}{\rightarrow} \\ \dot{i} \left[ \left( \frac{\partial g_{i''}}{\partial r_i} \right)^{-1} \right] \end{array} \right] \cdot \downarrow \left[ \begin{array}{c} \overset{i'}{\rightarrow} \\ \dot{i} \left[ \left( \frac{1}{\sigma_{i''}} \right)^0 \right] \end{array} \right] ; \quad \downarrow \left[ \begin{array}{c} \overset{i}{\rightarrow} \\ \dot{i} \left( \frac{1}{\sigma_{i''}} \right)^0 \end{array} \right] \downarrow \left[ \begin{array}{c} \overset{i''}{\rightarrow} \\ \dot{i} \left[ \left( \frac{\partial g_{i''}}{\partial r_i} \right)^{-1} \right] \end{array} \right] \quad (D-5)$$

At this point equation (D-2) has not been modified. The equation will be modified, however, by a change applied to the product factors of (D-5) where:

$$\downarrow \left[ \begin{array}{c} \overset{i''}{\rightarrow} \\ \dot{i} \left[ \left( \frac{\partial g_{i''}}{\partial r_i} \right)^{-1} \right] \end{array} \right] \quad (D-6)$$

is replaced by:

$$\downarrow \left[ \begin{array}{c} \overset{i''}{\rightarrow} \\ \dot{i} \left[ \left( \frac{\partial g_{i''}}{\partial r_i} \right)^{-1} \right] \end{array} \right] = \downarrow \left[ \begin{array}{c} \overset{i''}{\rightarrow} \\ \dot{i} \left[ \left( \frac{\partial G_{i''}}{\partial R_i} \right)^{-1} \right] \end{array} \right] \quad (D-7)$$

This means that in the function  $(\partial g_i''/\partial r_i)$  of (D-5), everywhere an  $r_i$  occurs replace it with  $R_i$  (i.e., a data value).

Now using equations (D-5), (D-6) and (D-7) define:

$$\downarrow \left[ \begin{array}{c} \stackrel{i''}{\rightarrow} \\ \left( \frac{\partial g_i''}{\partial r_i} \right)_{r=R}^{-1} \end{array} \right] \cdot \downarrow \left[ \begin{array}{c} \stackrel{i'}{\rightarrow} \\ \left( \frac{1}{\sigma_{ii}''} \right) \end{array} \right] = \downarrow \left[ \begin{array}{c} \stackrel{i''}{\rightarrow} \\ \left( \frac{1}{\sigma_{ii}''} \right)_{new} \end{array} \right] \quad (D-8)$$

And:

$$\downarrow \left[ \begin{array}{c} \stackrel{i''}{\rightarrow} \\ \left( \frac{1}{\sigma_{ii}''} \right) \end{array} \right] \downarrow \left[ \begin{array}{c} \stackrel{i'}{\rightarrow} \\ \left( \frac{\partial g_i''}{\partial r_i} \right)_{r=R}^{-1} \end{array} \right] = \downarrow \left[ \begin{array}{c} \stackrel{i''}{\rightarrow} \\ \left( \frac{1}{\sigma_{ii}''} \right)_{new} \end{array} \right] \quad (D-9)$$

where equation (D-8) and (D-9) contain only constants.

Substitution of equations (D-3) through (D-9) into equation (D-2) gives:

$$\left\{ \sum_{i=1}^n + \lambda \downarrow \left[ \begin{array}{c} \stackrel{i''}{\rightarrow} \\ \left( \frac{\partial g_i''}{\partial x_j} \right) \end{array} \right] \cdot \downarrow \left[ \begin{array}{c} \stackrel{i'}{\rightarrow} \\ \left( \frac{1}{\sigma_{ii}''} \right)_{new} \end{array} \right] \cdot \downarrow \left[ \begin{array}{c} \stackrel{i''}{\rightarrow} \\ \left( \frac{1}{\sigma_{ii}''} \right)_{new} \end{array} \right] \cdot \downarrow \left[ \begin{array}{c} \stackrel{j}{\rightarrow} \\ \left( \frac{\partial g_i''}{\partial x_j} \right) \end{array} \right] \right\} \cdot \downarrow \left[ \begin{array}{c} \stackrel{j}{\rightarrow} \\ \left( \Delta x_j \right) \end{array} \right] \quad (D-10)$$

Note that as the parameter " $\lambda$ " is increased in steps, the values of the  $r_i$ 's of equation (D-2) approach the values of the data values,  $R_i$ . That is, in equations (D-3) and (D-4):

$$\downarrow \left[ \begin{array}{c} \stackrel{i''}{\rightarrow} \\ \left( \frac{\partial g_i''}{\partial r_i} \right) \end{array} \right] \quad (D-11)$$

Approaches

$$\downarrow \left( \frac{\partial g_i}{\partial r_i} \right)_{r=R}^i = \downarrow \left( \frac{\partial G_i}{\partial R_i} \right) \quad (D-12)$$

as " $\lambda$ " becomes larger.

Thus the following product, implicit in equation (D-10),

$$\left\{ \downarrow \left[ \left( \frac{\partial g_i}{\partial r_i} \right)_{r=R}^i \right] \cdot \downarrow \left( \frac{\partial g_i}{\partial r_i} \right)_{r \rightarrow R}^i \right\} ; \left\{ \downarrow \left( \frac{\partial g_i}{\partial r_i} \right)_{r=R}^i \cdot \downarrow \left[ \left( \frac{\partial g_i}{\partial r_i} \right)_{r=R}^i \right] \right\} \quad (D-13)$$

approach the unit matrix as the  $r_i$ 's approach the  $R_i$ 's. Then, equation (D-10) will approach being the original left hand side of equation (D-1).

Now consider the right hand side of equation (D-1). This may be written as:

$$\left\{ \underbrace{C_{m \times l} \cdot \downarrow \left( x_i \right) - \downarrow \left( V_f \right) + \lambda \downarrow \left[ \frac{\partial r_i}{\partial x_j} \right] \cdot \underbrace{\left\{ \downarrow \left( \frac{\partial g_i}{\partial r_i} \right) \cdot \downarrow \left[ \left( \frac{\partial g_i}{\partial r_i} \right)^{-1} \right] \right\} \cdot \downarrow \left( \frac{\partial g_i}{\partial r_i} \right)}_{\text{unit matrix}} \right\} + \underbrace{\downarrow \left( \frac{\partial g_i}{\partial r_i} \right) \cdot \underbrace{\left\{ \downarrow \left( \frac{\partial g_i}{\partial r_i} \right) \cdot \downarrow \left( \frac{\partial g_i}{\partial r_i} \right) \right\} \cdot \downarrow \left( r_i - R_i \right)}_{\text{unit matrix}}}_{\text{unit matrix}} \quad (D-14)$$

Note in equation (D-14) that:

$$\downarrow \left[ \begin{array}{c} \overset{\leftarrow}{i} \\ \frac{\partial r_i}{\partial x_i} \end{array} \right] \cdot \downarrow \left( \frac{\partial g_i''}{\partial r_i} \right) = \downarrow \left[ \begin{array}{c} \overset{\leftarrow}{i} \\ \frac{\partial g_i''}{\partial x_i} \end{array} \right] \quad (D-15)$$

And

$$\downarrow \left( \frac{\partial g_i''}{\partial r_i} \right) \cdot \downarrow (r_i - R_i) \approx \downarrow \left( g_i'' - G_i'' \right) \quad (D-16)$$

Also consider the following products of equation (D-14):

$$\left\{ \downarrow \left[ \begin{array}{c} \overset{\leftarrow}{i} \\ \left( \frac{\partial g_i''}{\partial r_i} \right)^{-1} \end{array} \right] \downarrow \left( \frac{1}{e^{\sigma_{ii}}} \right) \right\} \circ \left\{ \downarrow \left( \frac{1}{e^{\sigma_{ii}}} \right) \downarrow \left[ \left( \frac{\partial g_i''}{\partial r_i} \right)^{-1} \right] \right\} \quad (D-17)$$

At this point, equation (D-14) has not been modified, except by way of approximation (D-16). Equation (D-14) is modified by the change applied to the product factors of (D-17) where:

$$\downarrow \left[ \begin{array}{c} \overset{\leftarrow}{i} \\ \left( \frac{\partial g_i''}{\partial r_i} \right)^{-1} \end{array} \right] \quad (D-18)$$

is replaced by:

$$\downarrow \left[ \left( \frac{\partial g_i''}{\partial r_i} \right)_{r=R}^{-1} \right] = \downarrow \left[ \left( \frac{\partial G_i''}{\partial R_i} \right)_{r=R}^{-1} \right] \quad (D-19)$$

Again, this means that in the function  $(\partial g_i'' / \partial r_i)$  of (D-17), everywhere an  $r_i$  occurs replace it with  $R_i$  (i.e., a data value).

Now using equations (D-17), (D-18) and (D-19) define:

$$\downarrow \left[ \left( \frac{\partial g_i''}{\partial r_i} \right)_{r=R}^{-1} \right] \downarrow \left( \frac{1}{C_i \sigma_{i''}^2} \right) = \downarrow \left( \frac{1}{\sigma_{i''}^2} \right)_{new} \quad (D-20)$$

and

$$\downarrow \left( \frac{1}{C_i \sigma_{i''}^2} \right) \downarrow \left[ \left( \frac{\partial g_i''}{\partial r_i} \right)_{r=R}^{-1} \right] = \downarrow \left( \frac{1}{\sigma_{i''}^2} \right)_{new} \quad (D-21)$$

where (D-20) and (D-21) contain only constants.

Substitution of equations (D-15) through (D-21) into equation (D-14) gives:

$$\left\{ \underset{\downarrow}{C}_{\text{model}} \cdot \underset{\downarrow}{\mathcal{L}}\left(\underset{\downarrow}{x_j}\right) - \underset{\downarrow}{\mathcal{L}}\left(\underset{\downarrow}{V_j}\right) + \lambda \underset{\downarrow}{\mathcal{L}}\left[\frac{\partial g_i''}{\partial x_j}\right] \cdot \underset{\downarrow}{\mathcal{L}}\left(\underset{\downarrow}{\frac{1}{C_{r_i}''}}\right) - \underset{\downarrow}{\mathcal{L}}\left(\underset{\downarrow}{\frac{1}{C_{r_i}''}}\right) \cdot \underset{\downarrow}{\mathcal{L}}\left(\underset{\downarrow}{g_i'' - \epsilon_i''}\right) \right\} \quad (D-22)$$

As discussed previously for the left hand side of equation (D-1), as the parameter " $\lambda$ " is increased in steps, the values of the  $r_i$ 's of the right hand side of equation (D-1) approach the values of the data values,  $R_i$ .

That is, from equation (D-15) and (D-16)

$$\underset{\downarrow}{\mathcal{L}}\left(\underset{\downarrow}{\frac{\partial g_i''}{\partial r_i}}\right) \quad (D-23)$$

approaches:

$$\underset{\substack{\downarrow \\ r=R}}{\mathcal{L}}\left(\underset{\downarrow}{\frac{\partial g_i''}{\partial r_i}}\right) = \underset{\substack{\downarrow \\ r=R}}{\mathcal{L}}\left(\underset{\downarrow}{\frac{\partial g_i''}{\partial R_i}}\right) \quad (D-24)$$

as " $\lambda$ " becomes larger.

Thus the following products, implicit in equation (D-14):

$$\left\{ \underset{\downarrow}{\mathcal{L}}\left[\left(\underset{\substack{\downarrow \\ r=R}}{\frac{\partial g_i''}{\partial r_i}}\right)^{-1}\right] \underset{\downarrow}{\mathcal{L}}\left(\underset{\substack{\downarrow \\ r=R}}{\frac{\partial g_i''}{\partial r_i}}\right) \right\} ; \left\{ \underset{\downarrow}{\mathcal{L}}\left(\underset{\substack{\downarrow \\ r=R}}{\frac{\partial g_i''}{\partial r_i}}\right) \underset{\downarrow}{\mathcal{L}}\left[\left(\underset{\substack{\downarrow \\ r=R}}{\frac{\partial g_i''}{\partial r_i}}\right)^{-1}\right] \right\} \quad (D-25)$$

approach the unit matrix as the  $r_i$ 's approach the  $R_i$ 's. Then equation (D-22) will approach being the original right hand side of equation (D-1).

Appendix E. The Derivatives,  $(\partial g_i' / \partial r_i)$ .

Appendix D makes no assumptions about the functional relationships between the vectors  $\vec{r}$  and  $\vec{g}$  (and hence  $\vec{R}$  and  $\vec{G}$ ) except that the derivatives  $(\partial g_i' / \partial r_i)$  must be definable.

From equation (97) of the main text:

$$\left( \frac{dr}{du} \right)_i = \sum_{L=1}^m (a_{iL}) r_L \quad (E-1)$$

Substituting equation (E-1) into equation (83) gives:

$$\begin{aligned} g_1 &= r_1 \\ g_{L'} &= 1/n \left( \frac{dr}{du} \right)_{L'} = 1/n \left\{ \sum_{L=1}^m (a_{L'}) r_L \right\} \quad (E-2) \\ & ; L' = 2, \dots, m \end{aligned}$$

Taking derivatives with respect to  $r_i$  and using the identity:

$$\frac{d\{1/n(u)\}}{dx} = \frac{1}{u} \frac{du}{dx} \quad (E-3)$$

Gives from equation (E-2):

$$\frac{\partial g_1}{\partial r_1} = 1 \quad ; \quad \frac{\partial g_1}{\partial r_L} = 0 \quad (E-4) \\ ; L = 2, \dots, m$$

and

$$\frac{\partial g_{L'}}{\partial r_i} = \frac{a_{iL'}}{\sum_{L''=1}^m (a_{iL''}) r_{L''}} \quad ; \quad L' = 2, \dots, m \quad ; \quad L = 1, \dots, m \quad (E-5)$$

and similarly for  $\vec{R}$  and  $\vec{G}$ .

The  $a_{i,i}$ 's (and the  $a_{i,i''}$ 's) are constants which depend only on the number of, and the spacing of, the frequencies,  $\omega_i$ .

## INITIAL DISTRIBUTION LIST

### Department of Defense

Assistant Secretary of Defense  
CMD, CONT, COMM & INTELL  
Department of Defense  
Washington, DC 20301  
01CY ATTN M. Epstein  
01CY ATTN J. Babcock

Director  
Command Control Technical Center  
Pentagon Rm BE 685  
Washington, DC 20301  
01CY ATTN C-650  
01CY ATTN C-312

Director  
Defense Advanced Research Project  
Agency  
Architect Building  
1400 Wilson Blvd.  
Arlington, VA 22209  
01CY ATTN Nuclear Monitoring Rsch  
01CY ATTN Strategic Tech. Office

Defense Communication Engineer Center  
1860 Wiehle Avenue  
Reston, VA 22090  
01CY ATTN Code R220 M. Horowitz  
01CY ATTN Code R720 John Worthington  
01CY Code R410 James W. McLean  
01CY Code R103

Director  
Defense Communications Agency  
Washington, DC 20305  
01CY ATTN Code 810 R. W. Rostron  
01CY ATTN Code 480  
01CY ATTN Code 101B MAJ Rood

Defense Communications Agency  
WMMCCS System Engineering Org  
Washington, DC 20305  
01CY ATTN R. L. Crawford

Defense Documentation Center  
Cameron Station  
Alexandria, VA 22314  
12CY ATTN TC

Director  
Defense Intelligence Agency  
Washington, DC 20301  
01CY ATTN DIAST-5  
01CY ATTN DIAAP Albert L. Wise  
01CY ATTN DB-4C Edward OFarrell  
01CY ATTN DT-1BZ CAPT R. W. Morton  
01CY ATTN HQ-TR J. H. Stewart

Director  
Defense Nuclear Agency  
Washington, DC 20305  
01CY ATTN DDST  
01CY ATTN TISI Archives  
03CY ATTN TITL Tech. Library  
03CY ATTN RAAE  
01CY ATTN STVL

Commander  
Field Command  
Defense Nuclear Agency  
Kirtland AFB, NM 87115  
01CY ATTN FCPR

Director  
Interservice Nuclear Weapons School  
Kirtland AFB, NM 87115  
01CY ATTN Document Control

Director  
Joint Strat TGT Planning Staff JCS  
Offutt AFB  
Omaha, NB 68113  
01CY ATTN JPST CAPT D. G. Goetz

Chief  
Livermore Division Fld Command DNA  
Lawrence Livermore Laboratory  
P.O. Box 808  
Livermore, CA 94550  
01CY ATTN FCPR

Director  
National Security Agency  
FT. George G. Meade, MD 20755  
01CY ATTN W65  
01CY ATTN Oliver H. Bartlett W32  
01CY ATTN Technical Library  
01CY ATTN John Skillman R52

OJCS/J-3  
The Pentagon  
Washington, DC 20301  
(Operations)  
01CY ATTN WMMCCS Eval OFC Mr. Toma

OJCS/J-5  
The Pentagon  
Washington, DC 20301  
(Plans & Policy)  
01CY ATTN Nuclear Division

Under Secry of Defense for Research  
and Engineering  
Department of Defense  
Washington, DC 20301  
01CY ATTN S&SS (OS)

Department of the Army

Commander/Director  
Atmospheric Sciences Laboratory  
US Army Electronics Command  
White Sands Missile Range, NM 88002  
01CY ATTN DELAS-AE-M F. E. Niles

Commander  
Harry Diamond Laboratories  
2800 Powder Mill Rd.  
Adelphi, MD 20783  
01CY ATTN DELHD-NP Francis N. Wimenitz  
01CY ATTN Mildred H. Weiner DRXDO-II

Commander  
US Army Electronics Command  
Fort Monmouth, NJ 07703  
01CY ATTN DRSEL-RD  
01CY ATTN J. E. Quigley

Commander  
US Army Foreign Science & Tech. Center  
220 7th Street, NE  
Charlottesville, VA 22901  
01CY ATTN R. Jones  
01CY ATTN P. A. Crowley

Commander  
US Army Nuclear Agency  
7500 Backlick Road  
Building 2073  
Springfield, VA 22150  
01CY ATTN MONA-WE J. Berberet

Chief  
US Army Research Office  
P.O. Box 12211  
Triangle Park, NC 27709  
01CY ATTN DRXRD-ZC

Department of the Navy

Chief of Naval Operations  
Navy Department  
Washington, DC 20350  
01CY ATTN OP 941  
01CY ATTN Code 604C3  
01CY ATTN OP 943 LCDR Huff  
01CY ATTN OP 981

Chief of Naval Research  
Navy Department  
Arlington, VA 22217  
01CY ATTN Code 402  
01CY ATTN Code 420  
01CY ATTN Code 421  
01CY ATTN Code 461  
01CY ATTN Code 464

Commanding Officer  
Naval Intelligence Support Center  
4301 Suitland Rd. Bldg. 5  
Washington, DC 20390  
01CY ATTN Code 5404 J. Galet

Commander  
Naval Ocean Systems Center  
San Diego, CA 92152  
01CY ATTN R. Eastman  
03CY ATTN Code 532  
01CY ATTN Code 532 William F. Moler

Director  
Naval Research Laboratory  
Washington, DC 20375  
01CY ATTN Code 5410 John Davis  
01CY ATTN Code 7701 Jack D. Brown  
01CY ATTN Code 5461 Trans. Iono. Prop.  
01CY ATTN Code 5465 Prop. Applications  
01CY ATTN Code 5460 Electromag. Prop. B  
02CY ATTN Code 2600 Tech. Library

Officer-in-Charge  
Naval Surface Weapons Center  
White Oak, Silver Spring, MD 20910  
01CY ATTN Code WA501 Navy Nuc Prgms Off  
01CY ATTN Code WX21 Tech. Library

**Commander**  
Naval Telecommunications Command  
NAVTELCOM Headquarters  
4401 Massachusetts Ave, NW  
Washington, DC 20390  
01CY ATTN Code 24C

**Commanding Officer**  
Navy Underwater Sound Laboratory  
Fort Trumbull  
New London, CT 06320  
01CY ATTN Peter Bannister  
01CY ATTN D. A. Miller

**Director**  
Strategic Systems Project Office  
Navy Department  
Washington, DC 20376  
01CY ATTN NSP-2141

**Department of the Air Force**

**Commander**  
ADC/DC  
ENT AFB, CO 80912  
01CY ATTN DC Mr. Long

**Commander**  
ADCOM/XPD  
ENT AFB, CO 80912  
01CY ATTN XPQDD  
01CY ATTN XP

**AF Geophysics Laboratory, AFSC**  
Hanscom AFB, MA 01731  
01CY ATTN CRU S. Horowitz  
01CY ATTN PHP Jules Aarons  
01CY ATTN OPR James C. Ulwick  
01CY OPR Alva T. Stair  
02CY SUOL Research Library

**AF Weapons Laboratory, AFSC**  
Kirtland AFB, NM 87117  
02CY ATTN SUL  
01CY ATTN SAS John M. Kamm  
01CY ATTN DYC CAPT L. Wittwer

**AFTAC**  
Patrick AFB, FL 32925  
01CY ATTN TN  
01CY ATTN TD-3  
01CY ATTN TD-5  
01CY ATTN TF/MAJ Wiley

**Air Force Avionics Laboratory, AFSC**  
Wright-Patterson AFB, OH 45433  
01CY ATTN AAD

**Commander**  
Foreign Technology Division, AFSC  
Wright-Patterson AFB, OH 45433  
01CY ATTN ETD B. L. Ballard

**HQ USAF/RD**  
Washington, DC 20330  
01CY ATTN RDQ  
**Headquarters**  
North American Air Defense Command  
1500 East Boulder  
Colorado Springs, CO 80912  
01CY ATTN Chief Scientist

**Commander**  
Rome Air Development Center, AFSC  
Griffiss AFB, NY 13440  
01CY ATTN EMTLD Doc. Library

**Commander**  
Rome Air Development Center, AFSC  
Hanscom AFB, MA 01731  
01CY ATTN EEP John Rasmussen

**SAMSO/MN**  
Norton AFB, CA 92409  
(Minuteman)  
01CY ATTN NMML LTC Kennedy

**Commander in Chief**  
Strategic Air Command  
Offutt AFB, NB 68113  
01CY ATTN NRT  
01CY ATTN XPFS MAJ Brian G. Stephan  
01CY ATTN DOK Chief Scientist

US Energy Research and Dev. Admin.

Department of Energy  
Albuquerque Operations Office  
P.O. Box 5400  
Albuquerque, NM 87115  
01CY ATTN Doc Con for D. W. Sherwood

Department of Energy  
Division of Headquarters Services  
Library Branch G-043  
Washington, DC 20545  
01CY ATTN Doc Con for Allen Labowitz

Division of Military Application  
Department of Energy  
Washington, DC 20545  
01CY ATTN Doc Con for Donald I. Gale

University of California  
Lawrence Livermore Laboratory  
P.O. Box 808  
Livermore, CA 94550  
01CY ATTN Glenn C. Werth L-216  
01CY ATTN Tech. Info Dept L-3  
01CY ATTN Frederick D. Seward L-46

Los Alamos Scientific Laboratory  
P.O. Box 1663  
Los Alamos, NM 87545  
01CY ATTN Doc Con for T. F. Taschek  
01CY ATTN Doc Con for D. R. Westervelt  
01CY ATTN Doc Con for P. W. Keaton  
01CY ATTN Doc Con for J. H. Coon

Sandia Laboratories  
Livermore Laboratory  
P.O. Box 969  
Livermore, CA 94550  
01CY ATTN Doc Con for B. E. Murphey  
01CY ATTN Doc Con for T. B. Cook ORG 8000

Sandia Laboratories  
P.O. Box 5800  
Albuquerque, NM 87115  
01CY ATTN Doc Con for Space Proj Div  
01CY ATTN Doc Con for A. D. Thornbrough  
ORG 1245  
01CY ATTN Doc Con for W. C. Myra  
01CY ATTN Doc Con for 3141 Sandia Rpt Coll

Other Government

Department of Commerce  
National Bureau of Standards  
Washington, DC 20234  
01CY ATTN Arthur Ernst  
01CY ATTN Raymond T. Moore

Department of Commerce  
Office of Telecommunications  
Institute for TELCOM Science  
Boulder, CO 80302  
01CY ATTN William F. Utlaud  
01CY ATTN L. A. Berry  
01CY ATTN A. Glenn Jean  
01CY ATTN D. D. Crombie  
01CY ATTN J. R. Wait

Department of Transportation  
Office of the Secretary  
TAD-44.1, Room 10402-B  
400 7th Street, SW  
Washington, DC 20590  
01CY ATTN R. L. Lewis  
01CY ATTN R. H. Doherty

Department of Defense Contractors

Aeronomy Corporation  
217 S. Neil Street  
Champaign, IL 61820  
01CY ATTN S. A. Bowhill

Aerospace Corporation  
P.O. Box 92957  
Los Angeles, CA 90009  
01CY ATTN Irving M. Garfunkel

Analytical Systems Engineering Corp.  
5 Old Concord Rd.  
Burlington, MA 01803  
01CY ATTN Radio Sciences

Boeing Company, The  
P.O. Box 3707  
Seattle, WA 98124  
01CY ATTN Glenn A. Hall  
01CY ATTN H. R. Willard  
01CY ATTN J. F. Kenney

University of California  
at San Diego  
Marine Physical Lab of the  
Scripps Institute of Oceanography  
San Diego, CA 92132  
01CY ATTN Henry G. Booker

Computer Sciences Corporation  
P. O. Box 530  
6565 Arlington Blvd  
Falls Church, VA 22046  
01CY ATTN D. Blumberg

University of Denver  
Colorado Seminary  
Denver Research Institute  
P. O. Box 10127  
Denver, CO 80210  
01CY ATTN Donald Dubbert  
01CY ATTN Herbert Rend

Develco  
530 Logue Avenue  
Mountain View, CA 94040  
01CY ATTN L. H. Rorden

ESL, Inc.  
495 Java Drive  
Sunnyvale, CA 94086  
01CY ATTN James Marshall

General Electric Company  
Space Division  
Valley Forge Space Center  
Goddard Blvd King of Prussia  
P. O. Box 8555  
Philadelphia, PA 19101  
01CY ATTN M. H. Bortner  
Space Science Lab.

General Electric Company  
TEMPO-Center for Advanced Students  
816 State Street  
P.O. Drawer QQ  
Santa Barbara, CA 93102  
01CY ATTN B. Gambill  
02CY ATTN DASIAC  
01CY ATTN Don Chandler  
01CY ATTN Warren S. Knapp

Geophysical Institute  
University of Alaska  
Fairbanks, AK 99701  
01CY ATTN T. N. Davis  
01CY ATTN Neal Brown  
01CY Technical Library

GTE Sylvania, Inc.  
Electronics Systems GRP  
Eastern Division  
77 A Street  
Needham, MA 02194  
01CY ATTN Marshal Cross

IIT Research Institute  
10 West 35th Street  
Chicago, IL 60616  
01CY ATTN Technical Library

University of Illinois  
Department of Electrical Engineering  
Urbana, IL 61803  
02CY ATTN Aeronomy Laboratory

Johns Hopkins University  
Applied Physics Laboratory  
Johns Hopkins Road  
Laurel, MD 20810  
01CY ATTN Document Librarian  
01CY ATTN J. Newland  
01CY P. T. Komiske

Lockheed Missiles & Space Co, Inc.  
3251 Hanover Street  
Palo Alto, CA 94304  
01CY ATTN E. E. Gaines  
01CY ATTN W. L. Imhof D/52-12  
01CY ATTN J. B. Reagan D/52-12  
01CY ATTN R. G. Johnson D/52-12

Lowell Research Foundation, Univ. of  
450 Aiken Street  
Lowell, MA 01854  
01CY ATTN Dr. Bibl

M.I.T. Lincoln Laboratory  
P.O. Box 73  
Lexington, MA 02173  
01CY ATTN Dave White  
01CY ATTN J. H. Pannell L-246  
01CY ATTN R. Enticknapp  
01CY ATTN D. M. Towle

Mission Research Corporation  
735 State Street  
Santa Barbara, CA 93101  
01CY ATTN R. Hendrick  
01CY ATTN F. Fajen  
01CY ATTN M. Scheibe  
01CY ATTN J. Gilbert  
01CY ATTN C. L. Longmire

Mitre Corporation  
P.O. Box 208  
Bedford, MA 01730  
01CY ATTN G. Harding

Pacific-Sierra Research Corp.  
1456 Cloverfield Blvd.  
Santa Monica, CA 90404  
01CY ATTN E. C. Field, Jr.

Pennsylvania State University  
Ionosphere Research Laboratory  
318 Electrical Engineering East  
University Park, PA 16802  
02CY ATTN Ionospheric Rsch Lab.

R&D Associates  
P.O. Box 9695  
Marina Del Rey, CA 90291  
01CY ATTN Forrest Gilmore  
01CY ATTN William J. Karzas  
01CY ATTN Phyllis Greifinger  
01CY ATTN Carl Greifinger  
01CY ATTN H. A. Ory  
01CY ATTN Bryan Gabbard  
01CY ATTN R. P. Turco

Rand Corporation  
1700 Main Street  
Santa Monica, CA 90406  
02CY ATTN Technical Library  
01CY ATTN Cullen Crain

SRI International  
333 Ravenswood Avenue  
Menlo Park, CA 94025  
01CY ATTN E. T. Pierce  
01CY ATTN Donald Neilson  
01CY ATTN George Carpenter  
01CY ATTN W. G. Chestnut  
01CY ATTN J. R. Peterson  
01CY ATTN Gary Price

Stanford University  
Radio Science Laboratory  
Stanford, CA 94305  
01CY ATTN R. A. Helliwell  
01CY ATTN R. Fraser-Smith  
01CY ATTN J. Katsufakis

TRW Defense & Space Sys. Group  
One Space Park  
Redondo Beach, CA 90278  
01CY ATTN Saul Altschuler  
01CY ATTN Dianna Dee